PONTIFICIA UNIVERSIDAD CATÓLICA DE CHILE
ESCUELA DE INGENIERÍA

DEVELOPING OF A HIGHLY STIFF AND DUCTILE REINFORCED CONNECTION CONCEPT WITH ENHANCED PINCHING FOR TIMBER STRUCTURES

RAÚL ALDO ANDRÉS ARAYA SEGOVIA

Thesis submitted to the Office of Research and Graduate Studies in partial fulfillment of the requirements for the Degree of Master of Science in Engineering

Advisor:
PABLO GUINDOS BRETONES

Santiago de Chile, January 2021

PONTIFICIA UNIVERSIDAD CATÓLICA DE CHILE
ESCUELA DE INGENIERÍA

DEVELOPING OF A HIGHLY STIFF AND DUCTILE REINFORCED CONNECTION CONCEPT WITH ENHANCED PINCHING FOR TIMBER STRUCTURES

RAÚL ALDO ANDRÉS ARAYA SEGOVIA

Members of the Committee:

PABLO GUINDOS BRETONES

HERNÁN SANTA MARÍA OYANEDEL

ALEXANDER OPAZO VEGA

JUAN CARLOS HERRERA MALDONADO

Thesis submitted to the Office of Research and Graduate Studies in partial fulfillment of the requirements for the Degree of Master of Science in Engineering

Santiago de Chile, January 2021

To the people who supported me and gave me their trust throughout this process.

AGRADECIMIENTOS

Quisiera partir agradeciendo al Departamento de Ingeniería y Gestión de la Construcción por disponer del curso de “Diseño y Construcción en Madera” durante el segundo semestre del año 2016, ya que correspondería a mi primer acercamiento al mundo de la madera, de la mano del profesor Mario Wagner, eminencia en lo que respecta al diseño con madera en Chile.

Sin embargo, el mayor agradecimiento se va por lejos a mi profesor supervisor Pablo Guindos. Su apoyo, guía y consejo a lo largo de toda esta investigación ha sido uno de los pilares fundamentales para el presente trabajo. Agradezco profundamente la confianza que él ha depositado en mí, en mis habilidades y en mi trabajo.

También me gustaría agradecer a todo el equipo del Centro de Innovación en Madera (CIM UC), en particular a Jairo Montaño, el che, por compartir tanto su experiencia en ensayos experimentales, como palabras de apoyo cuando las cosas no salían como estaban planificadas.

Finalmente, me gustaría agradecer a mi familia, mis hermanos Javier y Francisca; y mis padres Raúl y Marcela; quienes han sido un apoyo incondicional a lo largo de todo este trabajo. Agradezco también a mis amigos, compañeros, y en general a todas aquellas personas que han contribuido con palabras de apoyo, sobre todo durante este último tiempo donde todo resulta incierto producto de la pandemia.

TABLE OF CONTENTS

Page

LIST OF TABLES

Page

LIST OF FIGURES

Page

RESUMEN

En ingeniería de la madera, conexiones rígidas suelen estar acompañadas con penalizaciones en términos de ductilidad, sin mencionar problemas asociados al desempeño sísmico, como el pinching. Esta investigación presenta un nuevo concepto de refuerzo para conexiones titulado Gap Reinforced Fastened Connection (GRFC) que evita los problemas de rigidez-ductilidad y el pinching en la madera. El refuerzo se lleva a cabo mediante la adhesión vía epoxi de una placa de acero a la madera, luego se incorpora una segunda placa de acero distanciada un cierto gap respecto al plano de corte del conector. El mecanismo de falla consiste en forzar el desarrollo de las rótulas plásticas de los conectores al interior de este gap, evitando el aplastamiento de la madera, obteniendo un comportamiento dependiente solo de las propiedades de los conectores y de la interacción de estos con las placas de refuerzo. Los resultados experimentales han mostrado que, si bien el pinching no ha sido eliminado totalmente, este se reduce considerablemente. Esta reducción está directamente relacionada con el diámetro del conector utilizado, mostrando un mejor comportamiento mecánico para diámetros pequeños. Tanto los valores de rigidez como de ductilidad de la GRFC clavada fueron superiores a los valores de conexiones no reforzadas reportados en la literatura, alcanzando hasta 3.96 y 4.71 veces los valores de rigidez y ductilidad, respectivamente. La incorporación del GRFC permite reducir drásticamente el espaciamiento entre conectores, permitiendo utilizar los espaciamientos prescritos para acero, dado que el refuerzo elimina el riesgo de los efectos de grupo que desencadenan los modos de falla frágiles de la conexión. Mediante la incorporación del concepto GRFC se evita el típico trade-off entre rigidez y ductilidad de las conexiones de madera, permitiendo mejorar el rendimiento de conexiones rígidas que requieran una alta ductilidad, como por ejemplo las conexiones hold-down o de marcos de momento.

Palabras Claves: Conexiones de madera, rigidez, ductilidad, refuerzo, rótula plástica, comportamiento cíclico, pinching, espaciamiento, gap.

ABSTRACT

In timber engineering, high stiffness joints' requirements are usually accompanied by punishments in terms of ductility, not to mention problems associated with seismic performance such as pinching. This research presents a new reinforced connection concept entitled Gap Reinforced Fastened Connection (GRFC) that avoids both stiffness-ductility problems and pinching in the wood. The proposed reinforcement has been accomplished by incorporating a steel plate bonded with epoxy to the wood and separating another steel plate a certain gap at the shear plane. The failure mechanism consists of enforcing the development of plastic hinges of common fasteners at this gap interface, avoiding thus the crushing in the timber and obtaining a behavior dependent only on the properties of the connectors and their interaction with the reinforcement plates. Experimental results have shown that, although the entire pinching has not been eliminated, it has been considerably reduced. This reduction was directly related with the fastener's diameter, showing a better behavior for smaller diameters. Also, the stiffness and ductility of the nailed GRFC were superior to non-reinforced connection configurations reported in the literature, achieving up to 3.96 and 4.71 times stiffness and ductility values, respectively, using the same connection type. Another substantial improvement of the GRFC is that it allows to drastically reduce the fasteners' spacing because the reinforcement eliminates the risk of grouping effects that trigger brittle failure modes. In fact, it was found that the fasteners' spacing can be rather established according to that prescribed for steel structures. With the proposed reinforced connection concept, the traditional "trade-off" between stiffness and ductility of timber connections has been quantitatively surpassed. The presented connection is expected to greatly improve the performance of crucial connections in where both high stiffness and ductility are needed as for instance the hold-downs' connections or moment frame connections.

Keywords: Timber connection, stiffness, ductility, reinforcement, plastic hinge, cyclic behavior, pinching, spacing, gap interface.

1. INTRODUCTION

1.1 Thesis Structure

The thesis is divided into three chapters: the first one presents an introduction to the research. The second chapter is the main structure of the paper associated to this thesis, entitled “The Gap Reinforced Fastened Connection (GRFC): A highly stiff and ductile reinforced connection with enhanced pinching for timber structures”, submitted to the journal Engineering Structures on November 2020. The third chapter presents the conclusions of the research.

1.2 Background and problematic

In a structure, the joints are one of the critical factors in the design, regardless of the materiality of the structural elements that compose it, due to the mechanical requirements associated such as load-carrying capacity, stiffness, ductility, among others. Regarding the seismic performance of the connections, factors such as ductility and stiffness take on greater importance, in order to ensure the necessary deformation capacities. Such importance become even more evident for timber structures because, as opposed to steel structures, the plastic deformations are to be concentrated in the connections. The understanding and control of the plasticization in the structural elements has shown its benefits in the overall design of the structure; an example of this is the change in the design philosophy in steel moment frames post Northridge earthquake (Popov et al., 1998), where understanding in the development of plastic hinges became essential (Figure 1-2-1). In the same way, for timber and mass timber structures this understanding in the development of plastic hinges has been focused on the joints between timber members, and more precisely on parameters that are determining in its failure mechanisms, such as its geometry and type of fastener used (Schädle & Blaβ, 2011).

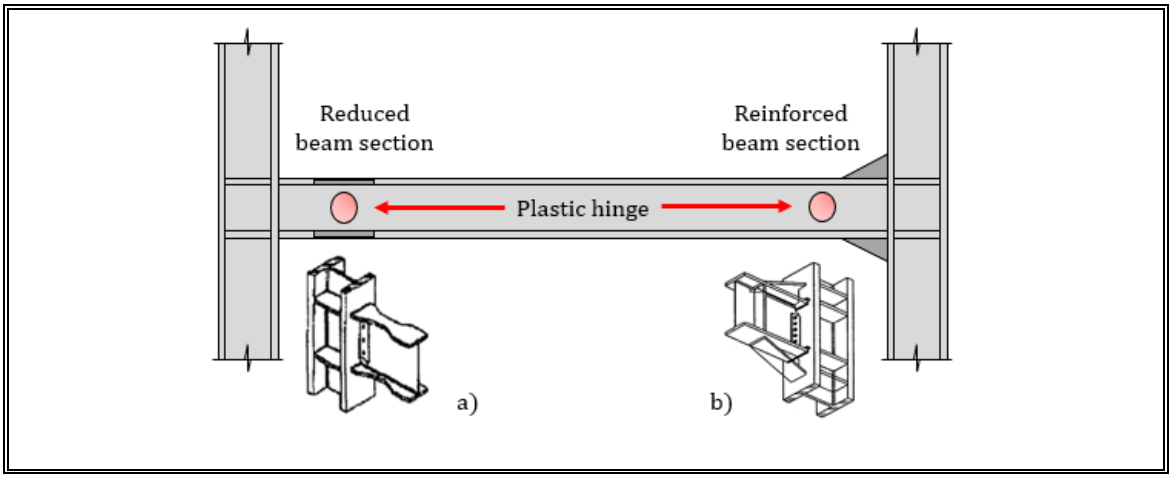

Figure 1-2-1: Typical plastic hinge forming mechanism in steel moment-resisting frames: a) Mechanism that induces formation of plastic hinges; b) Mechanism that prevents formation of plastic hinges

Multiple studies have been carried out in timber engineering over the years in order to characterize and possibly improve the stiffness and ductility of wooden connections. An example of this is the highly increasing utilization of self-tapping screws in crossed X-position, which achieves a moderate increase of load carrying capacity but a great improvement in terms of stiffness (up to 7 or more times stiffer in comparison to non-inclined fasteners' connections) because the deformation mechanism is mostly controlled by the axial extraction of the screws (Tomasi et al., 2010). However, such great improvement in the stiffness presents the drawback that is accompanied by a low ductility capacity against cyclic loads (Izzi & Polastri, 2019), making this connection impractical for being used as ductile connections in seismic countries. Other efforts on improving the stiffness-ductile behavior include the use of reinforcements transversal to the fasteners, which can be carried out by either using steel plates, where the plates are adhered by mechanical fixation like nail plates (Blaβ et al., 2000) and epoxy adhesives to the surfaces of the shear planes (Larson, 2019), or secondary screws (Figure 1-2-2) arranged transversely to the main fasteners, like Blaβ &

Schmid (2001) and Bejtka (2005). In both cases, the reinforcement provided by the inclusion of these metallic elements improved the ductile behavior and load-carrying capacity of the fastened connections and prevented brittle failure modes (Schädle & Blaβ, 2011). However, the stiffness of these connections were not greatly affected, and in the case of transverse fasteners' reinforcing, the beneficial effect of the reinforcement only takes place in one loading direction, but it does not provide an enhanced cyclic behavior.

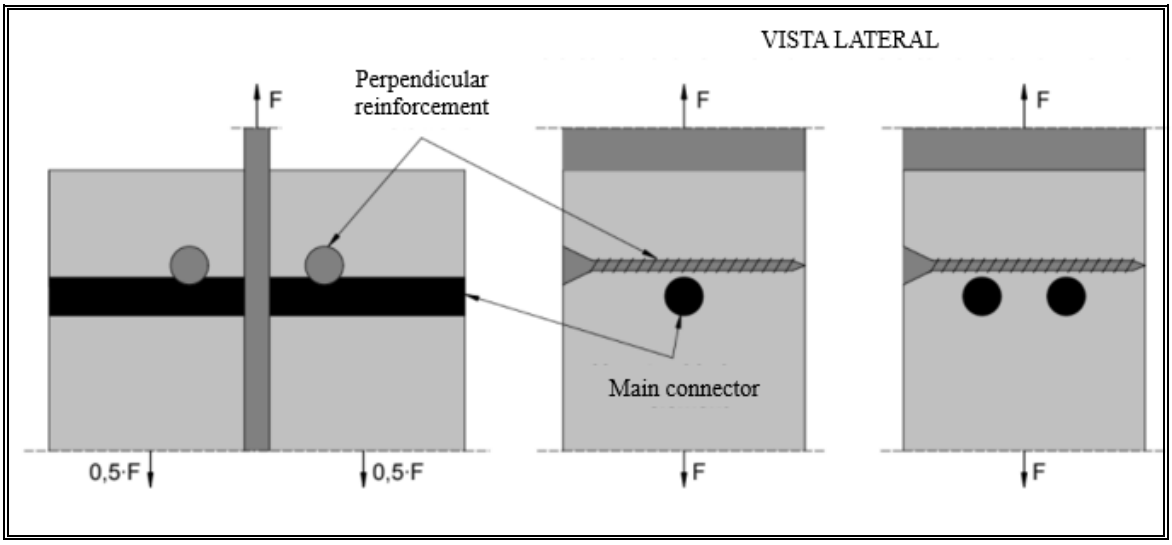

Figure 1-2-2: Perpendicular reinforcement with screws of the main connector, adapted from Bejtka (2005)

In fact, regarding to the cyclic behavior, the previous solutions were not aimed at improving the energy dissipation of the connection, which is why a stiffness degradation can be observed against cyclic loads (pinching effect), due to wood crushing. Examples of inventions focused towards energy dissipation increase have been generally focused on the development of new connectors, like Quenneville et al. (2018) or Scotta et al. (2016). However, many times the development of these new solutions focuses purely on the issue of energy dissipation, leaving aside key design concepts such as stiffness and

ductility. Solutions aimed at improving cyclic behavior were mostly focused on the use of metallic components, where dissipation occurs as a result of the relative displacements within the connection. Some examples of this are the U-shaped flexural plate developed by Kelly (1972); U-shaped plates arranged along a gap between timber panels that dissipate energy because of the flexion they undergo due to relative displacement of the panels (Figure 1-2-3). Furthermore, it has been seen that the use of steel plates as dowel-type fasteners could prevent pinching at the connection between panels (Blaβ & Schmidt, 2018), using the same principle of the U-shape plate. Those researches have however evidenced two important drawbacks for its practical utilization. The first being that very large inter-story drifts of about 2% and even 3% are necessary for these devices to provide the desired ductility and energy dissipation. Second, the utilization of gaps in between panels reduced up to 70% the lateral capacity of the connection in comparison to using the same connection hardware but without letting any gap at the shear plane.

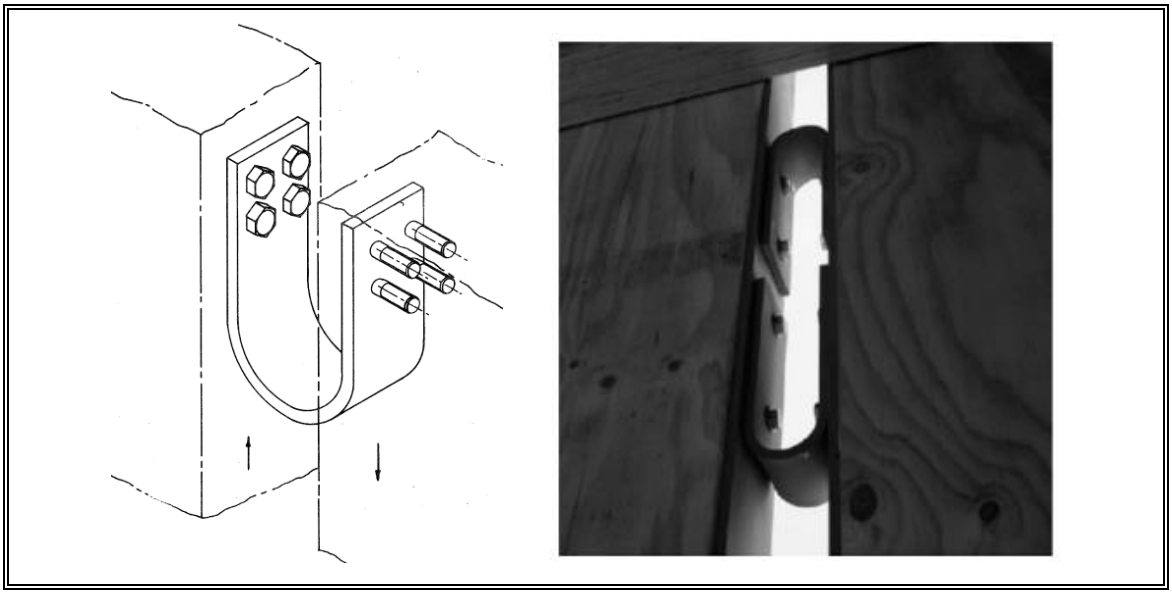

Figure 1-2-3: U-shaped flexural plates scheme (Kelly et al., 1972) and its application on timber structures (Blaβ & Schmidt, 2018)

In this research, a new connection entitled as Gap Reinforced Fastened Connection (GRFC) configuration is proposed. The GRFC concept can be applied to most conventional fasteners and the different monotonic and cyclic behavior is achieved by means of a steel plate reinforcement as well as a certain gap at the shear plane.

1.3 Objectives

The main objectives of this research are to develop the theoretical concept of a reinforced connection, which improves stiffness-ductility ratio, seismic behavior and fasteners spacing by incorporating a gap interface between the shear planes; and obtain an accurate mechanical characterization of the connections proposed through experimental tests.

2. THE GAP REINFORCED FASTENED CONNECTION (GRFC): A HIGHLY STIFF AND DUCTILE REINFORCED CONNECTION WITH ENHANCED PINCHING FOR TIMBER STRUCTURES

2.1 Theoretical development of the concept

As observed in Blaβ & Schmidt tests (2018), the incorporation of a physical interface (gap) between the surfaces of the shear plane improves the behavior of the hysteresis curve, where the repetitions of cycles are practically identical to the first cycle, eliminating the typical pinching effect of timber connections. However, these results were accompanied by losses in load-carrying capacity of up to 70%, which would imply the use of multiple fasteners to achieve load-carrying capacities like those that do not incorporate the gap (Figure 2-1-1). This loss of capacity is directly related to the physical measurement of the built-in gap, since it acts as an additional arm that, together with the shear loads acting on the fasteners, generates an additional moment on the fastener that reduces the load-carrying capacity. Although the above can be overcome by using more fasteners, this implies the use of larger timber elements to achieve the spacing requirements between fasteners in the connection area.

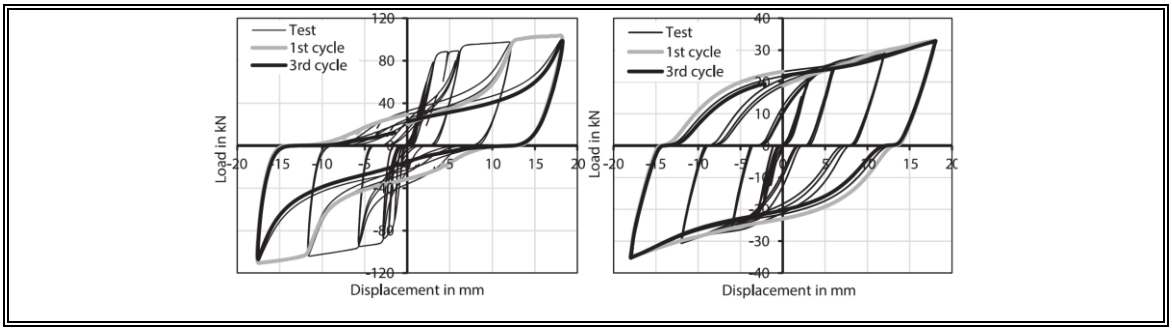

Figure 2-1-1: Load displacement curve for Blaβ & Schmidt test (2018). Hysteresis curve for connection without gap (left) and with gap (right).

The GRFC concept is based on incorporating the gap studied by Schmidt at the shear plane but using at the same time an epoxied steel plate reinforcement which completely changes the theoretical concept and mechanical behavior. For the GRFC, the gap would be set in-between steel plates, thus providing a physical space for the development of fixed plastic hinges at the fasteners. At the same time, the steel plates serve as a partial double embedment for the fasteners, where the crushing of the timber is replaced by the bearing of the steel. This replacement in the failure mechanism provides two crucial benefits: an increase in ductility as a result of the perpendicular reinforcement provided by the plate-fastener interaction (Blaβ et al., 2000; Blaβ & Schmid, 2001; Bejtka, 2005) and the reduction of spacings. For practical purposes, the scope of this article is limited to the study of GRFC for thick steel plates as reinforcements and single shear arrangements.

2.1.1 Failure modes

Mechanical characterization for timber joints, such as load-carrying capacity or stiffness, is carried out according to the failure modes proposed by Johansen (1949), also known as the european yield model, implemented in Eurocode 5, EN 1995 (European Committee for Standardization, 2010). These failure modes represent all possible limit states to which the fastener will possibly be subjected, such as brittle and ductile failures. This is accomplished by idealizing the free-body diagrams of the different failure modes by assuming infinitely stiff fasteners and, for the ductile failure modes, perfect plasticity upon yielding moments. For GRFC with one shear plane, six different possible failure modes are expected. These six failure mechanisms can be classified as undesirable or desirable.

Undesirable failure modes (Figure 2-1-2) relate to the brittle failure of any of the connection components, such as the steel plate reinforcement, fastener shear-off, or failure of the epoxy interface, whereas desirable modes are relate to ductile failure of the

fastener and the development of plastic hinges, see Figure 2-1-3. In Figure 2-1-3a, the embedment strength in the steel reinforcement is exceeded such that one of the plastic hinges is developed inside the timber member. In case that the embedment strength surpasses the flexural yielding of the fastener, then the failure mode evolves to the formation of both plastic hinges at the gap as illustrated in Figure 2-1-3b.

Based on the free-body diagrams, the load-carrying capacity (F_v) can be estimated according to the yielding failure model with Equations 2.1.1 - 2.1.6, where m is the gap thickness, d is the fastener diameter, f_{adh} is the adhesion tension, w is the penetration depth inside timber member, f_h is the embedment strength in the timber member, f_s is the embedment strength of the reinforcement, f_u is the shear strength of the fastener, s is the reinforcement (internal plate) thickness, t is the external plate thickness and M_y is the fastener yielding moment. If there is no gap (m = 0), Equation 2.1.5 yields to the EYM design expression for steel-to-timber joint with thick external steel plates (Blaβ & Sandhaas, 2017). When the embedment strength in timber reinforcement is exceeded, the plastic hinge is developed inside the timber member, producing pinching effect.

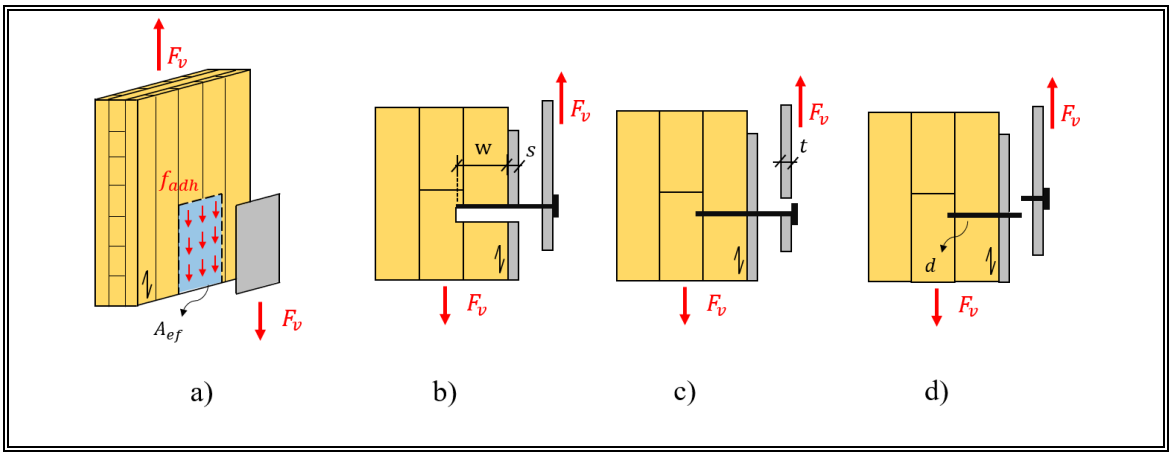

Figure 2-1-2: Undesirable failure modes: a) Epoxy interface failure; b) Timber-steel composite failure; c) Yielding of external steel plate; d) Fastener shear-off

$$F_{v,a} = f_{adh} \cdot A_{ef} \quad , \quad \text{Epoxied interface failure} \qquad (2.1.1)$$

$$F_{v,b} = f_h wd + f_s sd \quad , \quad \text{Timber-steel composite failure} \qquad (2.1.2)$$

$$F_{v,c} = f_s td \quad , \quad \text{External steel plate yielding} \qquad (2.1.3)$$

$$F_{v,d} = f_u 0.25\pi d^2 \quad , \quad \text{Fastener shear-off} \qquad (2.1.4)$$

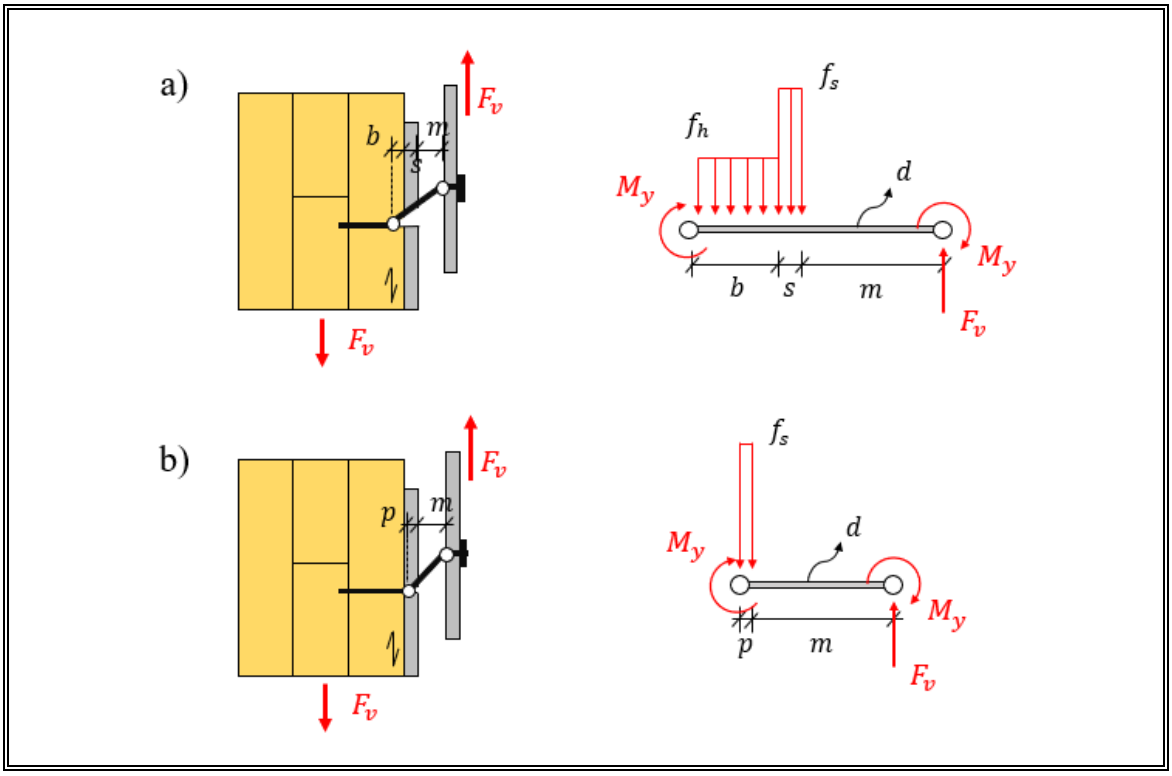

Figure 2-1-3: Free-body diagram of the single shear fastener: a) Plastic hinge development inside the timber element; b) Plastic hinge development inside the steel plate

$$F_{v,a} = f_h db + f_s sd \quad , \quad b = \left\{\sqrt{\frac{4M_y}{f_h d} - \{s^2 + 2sm\}\left(\frac{f_s}{f_h} - 1\right) + m^2} - (s + m)\right\} \qquad (2.1.5)$$

$$F_{v,b} = f_s dp \quad , \quad p = \left\{\sqrt{\frac{4M_y}{f_s d} + m^2} - m\right\} \qquad (2.1.6)$$

In the subsequent sections, the stiffness of the GRFC shall be estimated from an assumption of double embedment of the fasteners (Equation 2.1.6). Under this assumption, the reinforcing steel plates serve as an embedment surface, which allows for calculating the stiffness of GRFC assuming a parallel spring model, where the stiffness of each fastener shall match with the stiffness of an embedded frame element (typical $12EI/L^3$), whose element length equates the gap thickness (m).

2.1.2 Influence of reinforcement thickness and fastener diameter

An analytical sensitivity analysis was performed beforehand for different values of reinforcing plate thickness (s) and fastener diameter (d) in order to design the experimental characterization of the GRFC concept and elucidate the occurrence of different failure modes, which is shown in Figure 2-1-4.

The analysis of the reinforcing plate thickness was performed assuming 10D nails as fasteners and an external plate thickness of t = 4 mm (Figure 2-1-4a). The results showed that as s increases, the lateral load-carrying capacity increases proportionally. However, the gap thickness (m) required to keep plastic hinges developing away from timber (Equation 2.1.6) instead of yielding within the timber members (Equation 2.1.5) is not proportional: for s = 1 mm, the required m is 8.3 mm for hinges to develop at the reinforcement; while for s = 2 and 4 mm the required m reduce to 3.4 mm and 0.1 mm, respectively, see Figure 2-1-4a. On the other hand, the influence of d in the lateral capacity and failure modes' occurrence is shown in Figure 2-1-4b, which was analyzed assuming s = 3 and t = 4 mm. As shown in Figure 2-1-4b, the plastic hinge approaches the timber member as d increases due to reinforcement's embedment, requiring larger m to keep the plastic hinges away from timber. For larger d, the failure mechanism may eventually switch to undesirable external plate yielding (represented by the dotted line in Figure 2-1-4b), according to the Equation 2.1.3.

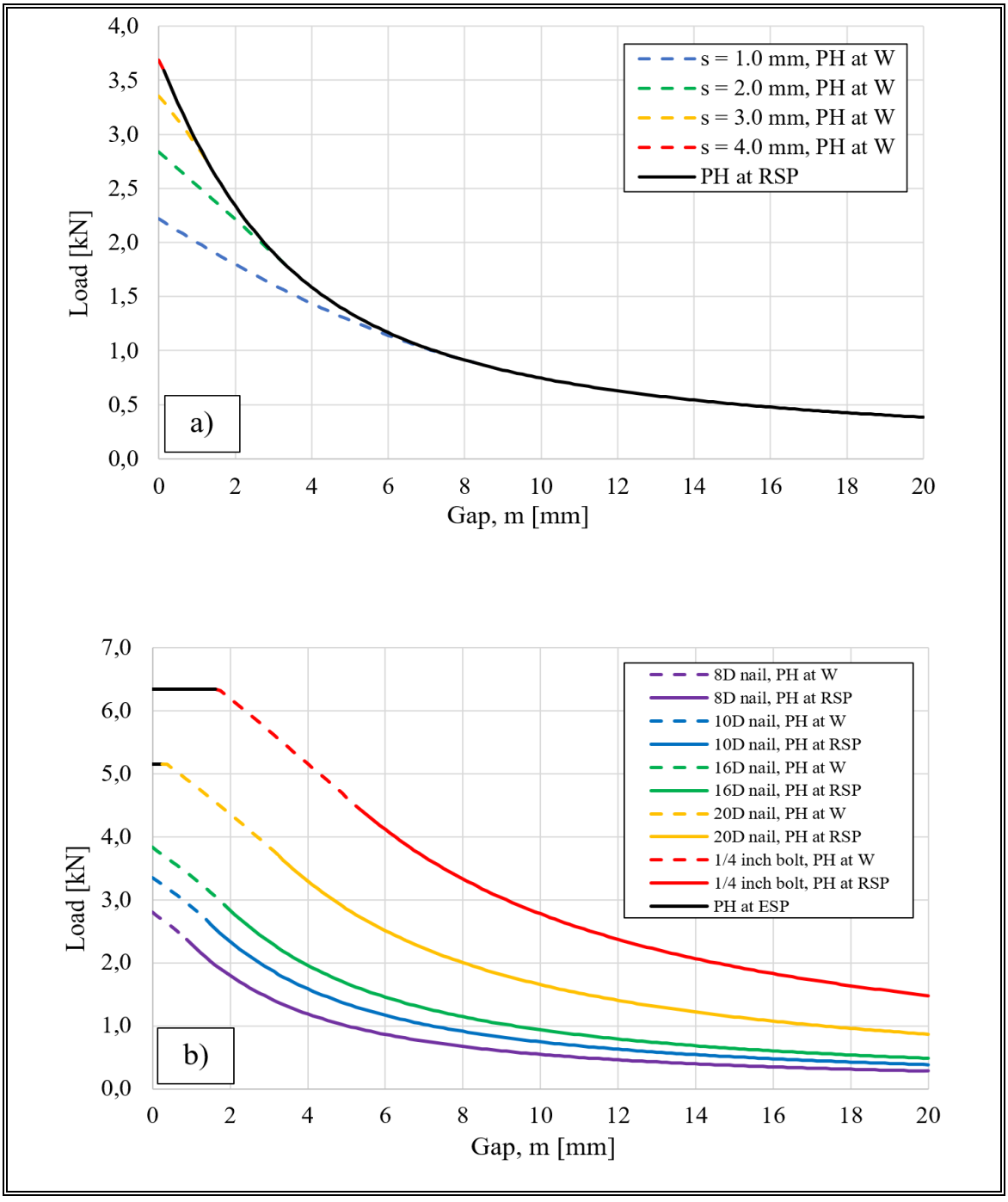

Figure 2-1-4: Analytical influence of: a) reinforcing steel plate thickness, s; b) fastener diameter, d; on the lateral capacity and occurrence of failure modes for GRFC when varying the gap thickness, m. (PH: Plastic hinge, RSP: Reinforcement steel plate, W: Wood, ESP: External steel plate)

2.2 Materials and methodology

The methodology used to determine mechanical properties of connections is the experimental monotonic and cyclic test of specimens, followed by an analysis of the recorded data. Details of the specimens, the test and the measurement procedure are detailed below.

2.2.1 Test specimens

The GRFC concept was characterized experimentally using reinforcing plates in hold-down type connections with a gap interface (HDG). Each specimen was fabricated with a 3-layer Chilean Radiata pine CLT (33-34-33 mm) manufactured at Forestal Tricahue Ltda., Concepción, Chile, with a total thickness of 100 mm, and two HDG connections, which were manufactured at the Laboratory of Structural Engineering of the Pontifical Catholic University in Santiago, Chile, using common A36 structural steel, see Figure 2-2-1. Both the reinforcing and external plates were made using perforated 4 mm thick steel plates. The perforations were made for 10D common nails (3.76 mm in diameter and 76.2 mm in length) using a longitudinal spacing and edge distance of 4D. In order to match the lateral capacity of the own produced HDG connection with that of a typical commercial hold down connection, such as for instance the HTT5 produced by Simpson Strong-Tie (Simpson Strong-Tie, 2019), 14 nails were used. The plates were drilled with a drill with a diameter equal to that of the nails, so that there was no clearance in the holes. A rigid bonding interface between the inner reinforcing plate and the CLT was generated by using Sikadur31 epoxy, produced by Sika Chile. Steel separator elements were welded to the external plate in order to generate the gap. While these elements do not fulfill a structural function in the connection, they are used to ensure the stability of the gap thickness (m) even after yielding of the fasteners. The dimensions of the specimens are presented in Figure 2-2-1.

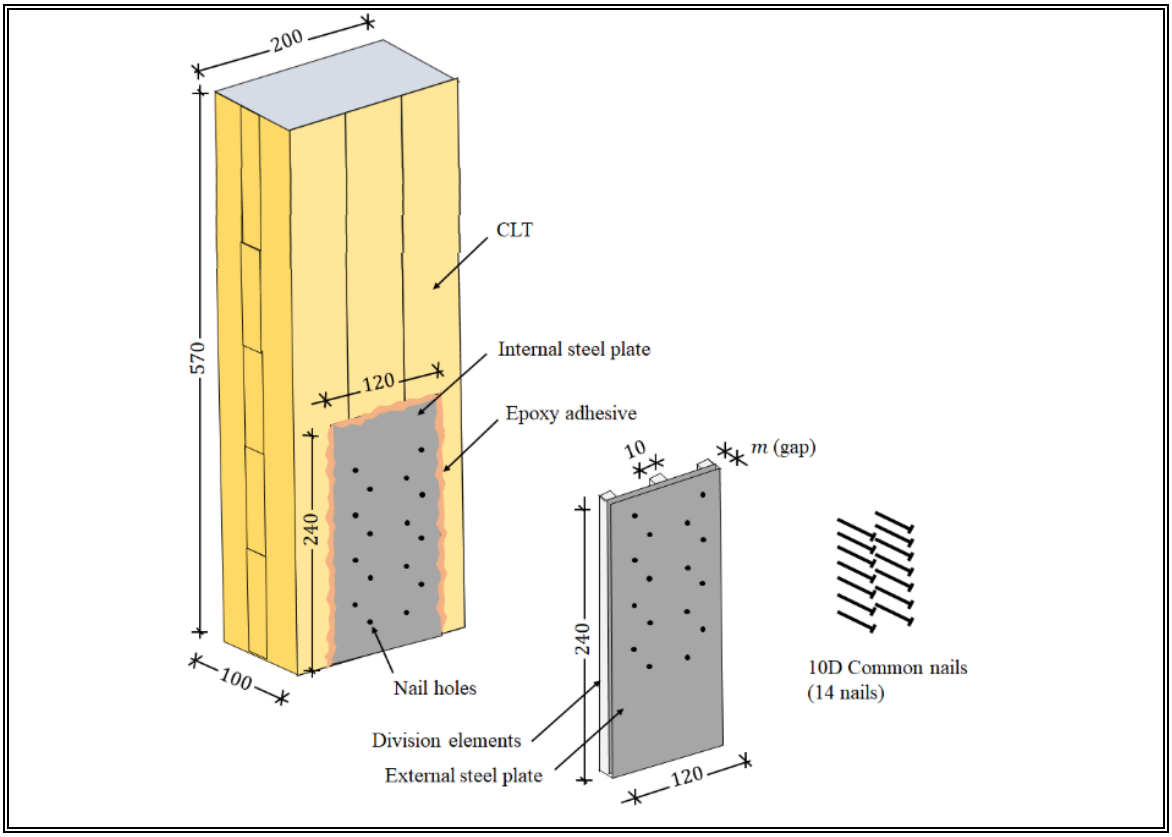

Figure 2-2-1: HDG connection scheme, distances in mm

The testing matrix for the HDG characterization is shown in Table 2-2-1. As shown in the table, five monotonic tests with varying gap size between 8 and 14 mm were performed with nail fasteners. For comparison purposes, a sixth monotonic test with 1/4" bolts was also accomplished. For cyclic testing a 8 mm gap was selected, and the variation was focused on the fastener type (nails and bolts), diameter and spacing. All specimens were designed with similar load-carrying capacity. The tag of specimens contains: the loading protocol (M for monotonic, C for cyclic), type of fastener (N for nail, B for bolts), gap thickness and a number that indicates spacing or diameter for cyclic tests.

Table 2-2-1: Test matrix for the specimens

Test	Loading*	Gap [mm]	Fastener	Diameter [mm]	Spacing**	n° fastener
MN-08	M	8	Nail	3.76	4D	28
MN-10	M	10	Nail	3.76	4D	28
MN-12	M	12	Nail	3.76	4D	28
MN-14	M	14	Nail	3.76	4D	28
MB-08	M	8	Bolt	6.35	6D	4
CN-08-1	C	8	Nail	3.76	4D	28
CN-08-2	C	8	Nail	3.23	4D	40
CB-08-1	C	8	Bolt	6.35	6D	4
CB-08-2	C	8	Bolt	6.35	3D	4

* M: Monotonic / C: Cyclic

** Longitudinal and edge spacing

Recorded density values for the test specimens are available in Appendix A.

2.2.2 Test setup

The test setup consisted of a typical double shear-plane symmetric connection set up as shown in Figure 2-2-2. The external steel plates of each specimen were welded to a 30 mm thick steel plate, which was bolted to the reaction slab. The vertical load was applied by an hydraulic actuator and transmitted to the timber by steel plates and dowels. Two LVDTs were used to measure vertical displacements in each side of each specimen: one for relative displacement between external and reinforcing plate, and the other for the displacement between reinforcing plate and CLT member. This configuration was used for both monotonic and cyclic tests, so a bidirectional load cell was used.

More specific details regarding the instrumentation are available in Appendix B.

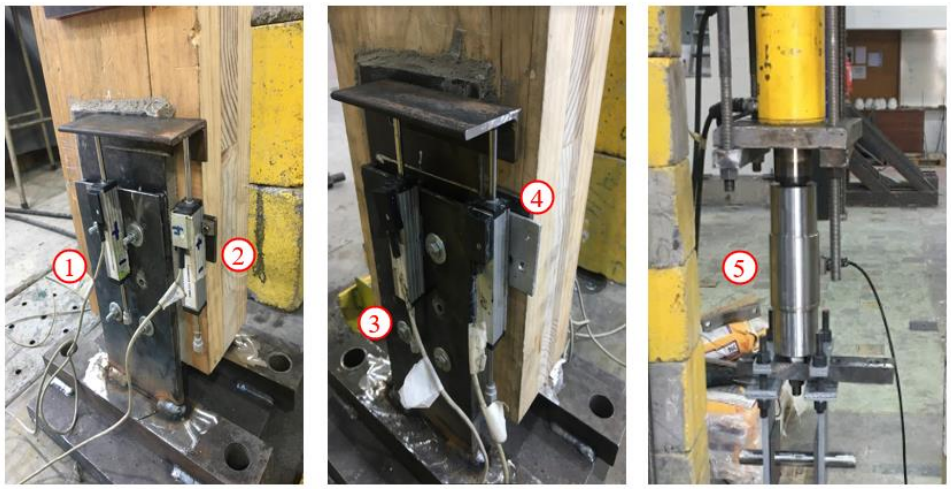

1 - Relative displacement between left plates
2 - Zero control between internal left plate and CLT
3 - Relative displacement between right plates
4 - Zero control between internal right plate and CLT
5 - Monotonic/Cyclic load application

Figure 2-2-2: Experimental setup for connection tests

2.2.3 Test procedure

The monotonic and cyclic tests were conducted using monotonic and reverse cyclic procedures with controlled displacement in accordance with the EN 12512 loading protocol for cyclic testing of joints made with mechanical fasteners (European Committee for Standardization, 2005). For monotonic tests, the test was executed by pulling up to failure of the connection or when the load-carrying capacity decreased to 80% of the maximum value reached. The calibration of protocol for the cyclic tests was carried out using the experimental yield values obtained from the monotonic tests, which varied depending on the configuration of each specimen. Figure 2-2-3 shows the normalized displacement protocol of EN 12512.

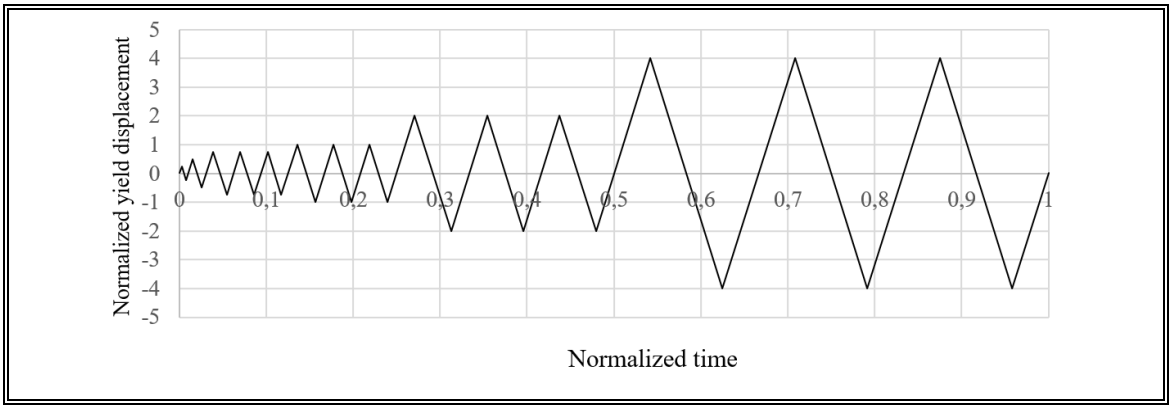

Figure 2-2-3: EN 12512 normalized protocol for cyclic tests

2.3 Results and discussion

2.3.1 Monotonic performance

The experimental results and discussion for the monotonic tests of the MN-08, MN-10, MN-12, MN-14 and MB-08 specimens are shown. Appendix C show the individual results of each test.

2.3.1.1 Load-carrying capacity

The monotonic tests' load-displacement results are presented in Figure 2-3-1 for different gap thicknesses. The load-carrying capacity was estimated as the maximum load recorded. For nailed (N) specimens with 8 mm, 10 mm, 12 mm and 14 mm gap thickness, the load-carrying capacity was 64.5 kN, 57.8 kN, 46.8 kN and 47.8 kN, respectively. The bolted (B) specimen with 8 mm gap size withstood 50.6 kN.

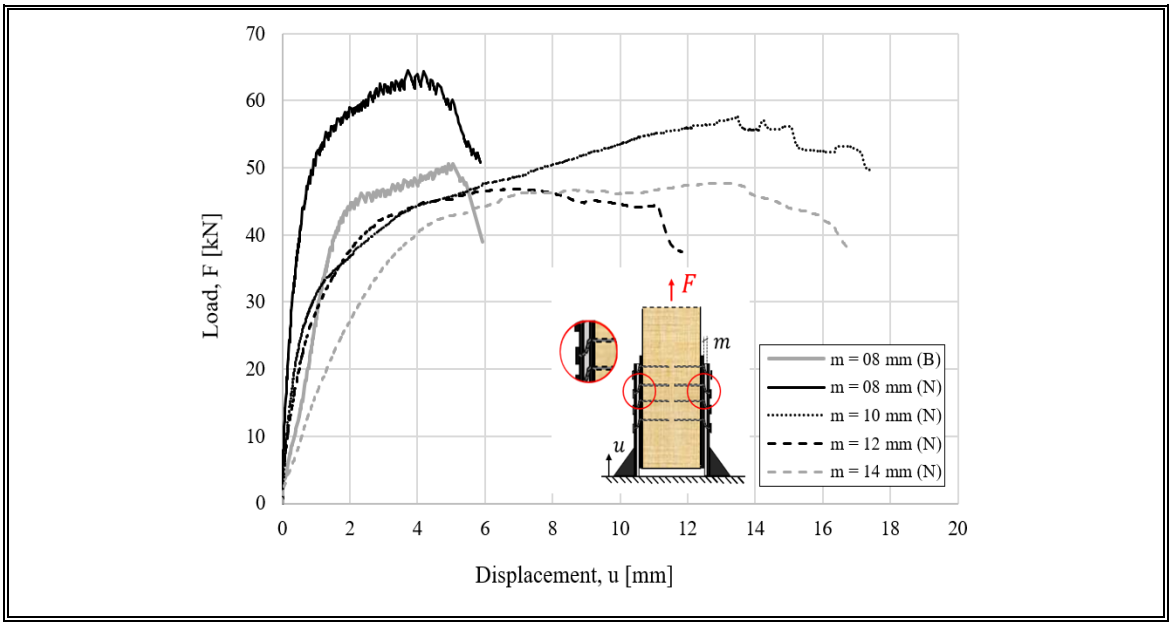

Figure 2-3-1: Load displacement curves for different gap sizes (m) and fasteners (B: ¼-inch bolted; N: 10D common nail)

2.3.1.2 Elastic stiffness

The elastic stiffness was calculated according to standard procedure of EN12512, i.e., is estimated as the slope between the load-displacement points for load levels equal to 10% and 40% of the measured load-carrying capacity. For comparison purposes, the elastic stiffness was also calculated with the EEEP method, considering the slope between zero and the load-displacement point at 40% of load-carrying capacity (American Society of Civil Engineers, 2012). For nailed (N) specimens with 8 mm, 10 mm, 12 mm and 14 mm gap size, the EN 12512 stiffness measured 89.4 kN/mm, 42.1 kN/mm, 33.6 kN/mm and 14.0 kN, respectively, whereas the EEEP stiffness measured 107.7 kN/mm, 48.3 kN/mm, 42.7 kN/mm and 15.4 kN/mm, respectively. The bolted (B) specimen with 8 mm gap size recorded a stiffness of 24.2 kN/mm according to EN 12512, and 26.3 kN/mm according to the EEEP method. The values are summarized in Table 2-3-1.

2.3.1.3 Ductility

The ductility was calculated as u_f/u_y, where the yielding displacement (u_y) was estimated according to the EN 12512 procedure (Figure 2-3-2b) - for comparison purposes, the yielding displacement was also estimated by the EEEP method (Figure 2-3-2a) -, and the failure displacement (u_f) was estimated as the displacement when load-carrying capacity decreased to 80% of the maximum value. For the nailed specimens (N), with 8 mm, 10 mm, 12 mm and 14 mm gap size, the ductility values were 13.3; 28.3; 14.5 and 6.6, respectively. The value obtained for the bolted specimen (B) was 3.53. Ductility values obtained for nailed connection estimated by EEEP method for 8 mm, 10 mm, 12 mm and 14 mm gap size were 10.9; 16.9; 11.7 and 5.8, respectively. Finally, ductility value for bolted specimen by EEEP method was 3.3.

Yielding parameters calculation for EN 12512 procedure and EEEP method is show in Appendix D.

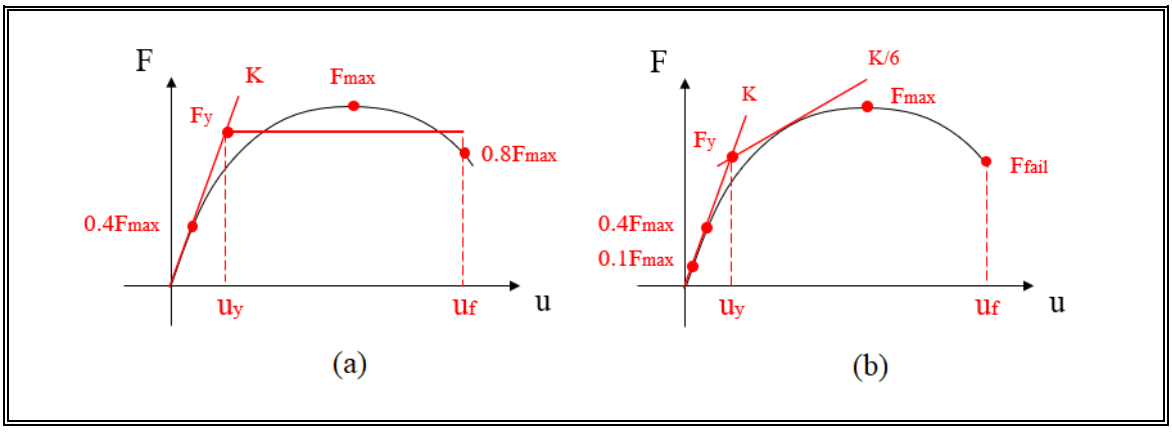

Figure 2-3-2: Estimation of yielding parameters: a) ASTM E2126-11: EEEP-Method; b) DIN EN 12512: 1/6-Method

2.3.2 Analysis and discussion of the monotonic performance

A summary of the most relevant monotonic measurements is shown in Table 2-3-1. The monotonic results confirm the dependence of the load-carrying capacity, stiffness, and ductility according to the gap thickness. An analytical comparison of the experimental results is made with the proposed ductile failure modes (Eq. 2.1.5 – Eq. 2.1.6). The estimation of yielding parameters is carried out from Eurocode 5 specifications, considering the following nominal values: d = 3.76 mm nail diameter, ρ_k = 370 kg/m^3 density for radiata pine (characteristic density value), f_{hk} = 29.2 MPa for embedment strength of the reinforcement, f_s = 235 MPa for embedment strength of reinforcement and f_u = 414 MPa for shear strength; obtaining a yielding moment of M_y = 3887 Nmm. Load-carrying capacity results in Figure 2-3-3c show that the design loads estimated by the proposed failure modes behave according to the experimental results, such that the difference in the magnitudes of the values shown in Figure 2-3-3b can be attributed to the typical safety factor on the design values, which in this case would

average 2.77 using its yielding parameters. When normalizing the load-carrying capacities according to the value obtained for an 8 mm gap size, it is obtained that the analytical results do not vary by more than 15% respect to the experimental results, which demonstrates the validity of the proposed analytical equations.

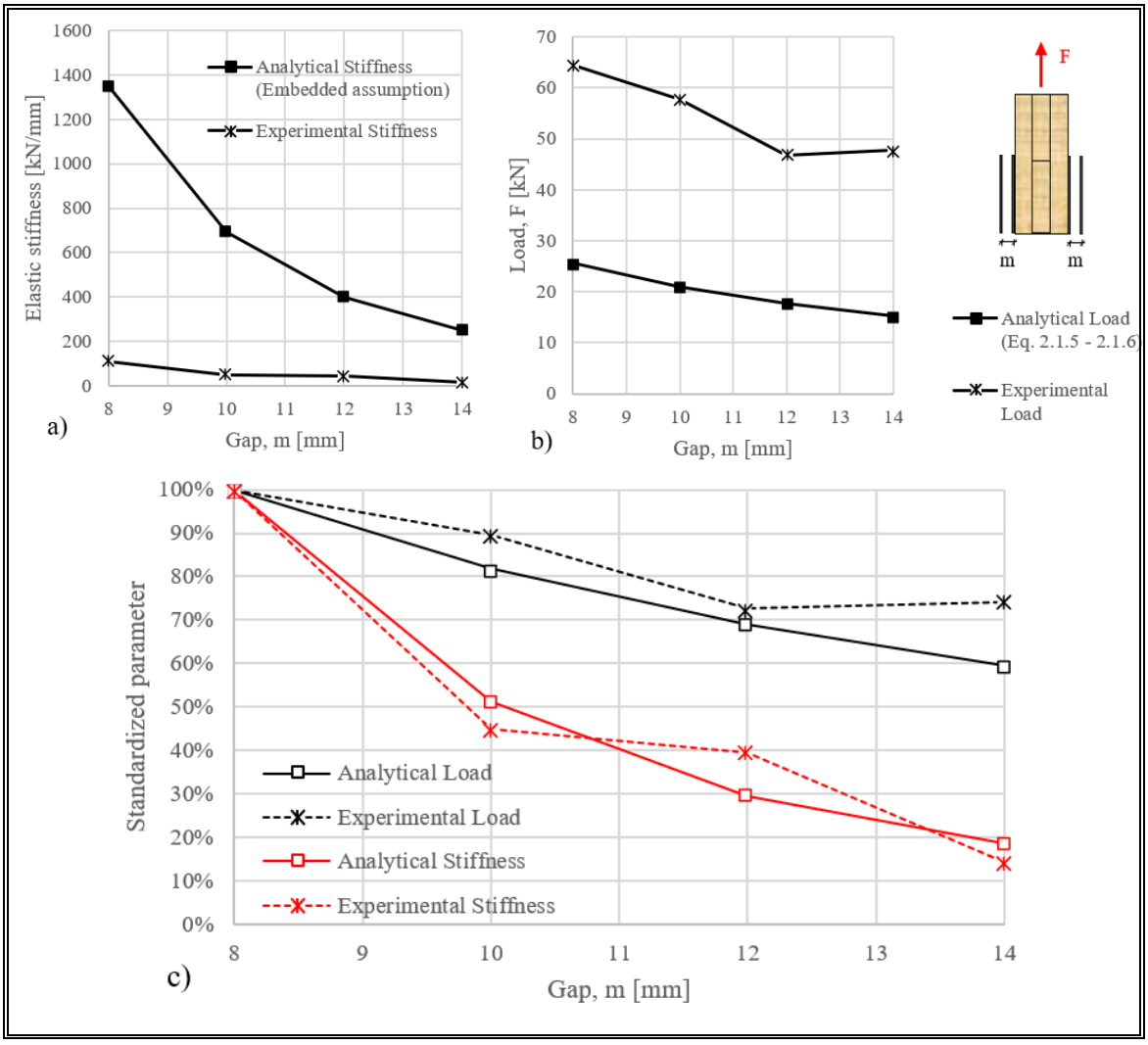

Figure 2-3-3: Connection tests comparison: a) Comparison between analytical and experimental stiffness; b) Comparison between analytical and experimental load-carrying capacity; c) Comparison of standardized parameters according to m = 8 mm

Table 2-3-1: Monotonic features of the HDG

Test	Gap	F_{max}	u_f	EN12512				EEEP			
				$K_{10-40\%}$	u_y	F_y	D	$K_{40\%}$	u_y	F_y	D
	[mm]	[kN]	[mm]	[kN/mm]	[mm]	[kN]	[-]	[kN/mm]	[mm]	[kN]	[-]
MB-08	8	50.6	5.93	24.2	1.68	42.3	3.5	26.3	1.78	46.8	3.3
MN-08	8	64.5	5.86	89.4	0.44	43.6	13.3	107.7	0.54	57.8	10.9
MN-10	10	57.8	17.41	42.1	0.62	28.9	28.3	48.3	1.03	49.6	16.9
MN-12	12	46.8	11.84	33.6	0.82	31.4	14.5	42.7	1.01	43.2	11.7
MN-14	14	47.8	16.72	14.0	2.55	37.4	6.6	15.4	2.88	44.4	5.8

Experimental stiffness values showed to be considerably lower than those estimated by the analytical assumption of double embedment for fasteners ($12EI/L^3$, where L is the gap m), reaching just 10% of its value. Such great divergence between analytical and experimental stiffness is attributed to the incapability of the reinforcing plates to act as a perfect embedment surface, causing the fasteners to rotate around contact area with the steel plates and thus distorting the idealization of the reinforcing plate as a fixed end. However, when normalizing the results according to the value obtained for an 8 mm gap thickness, the analytical results do not vary by more than 10% respect to the experimental results, which demonstrates that the proposed analytical expression still may be used to predict stiffness if considering a flexibilization factor of 0,1 due to a loss of the fixed end condition at the reinforcing plate, such that

$$K_{ser,GRFC} = \frac{1{,}2 \cdot EI}{m^3} \approx 0.059 \frac{E \cdot d^4}{m^3} \tag{2.3.1}$$

Equation 2.3.1 can be compared with the conventional stiffness equation proposed by the EN 1995-1 for nails

$$K_{ser,EN1995} = \frac{\rho_m^{1,5} \cdot d^{0,8}}{30} \tag{2.3.2}$$

The relationship of the conventional EN1995 stiffness and GRFC stiffness for a given 3.76 mm nail is shown in Figure 2-3-4. This analytical comparison, considering a

typical scenario in which the average density is about ρ_m = 420 kg/m^3 and the Young's modulus of the nails is E = 200 GPa, is consistent with the experimental results. For the tested specimens of m = 8 mm, 10 mm, 12 mm and 14 mm, the GRFC stiffness multiplied by factors of 3.96, 1.78, 1.57 and 0.57 the stiffness of a conventional HTT5 hold-down without GRFC, where stiffness is 13.61 kN/mm (Liu & Lam, 2019). Figure 2-3-4 also shows the experimental stiffness increase of a GRFC as a function of m. These theoretical and analytical relations are applicable only for nails, since the bolted specimen reached stiffness values of just 0.88 times the stiffness of a conventional connection. Such drop of stiffness is attributed to the embedment of the reinforcing plate, which was unable to increase the stiffness of the GRFC.

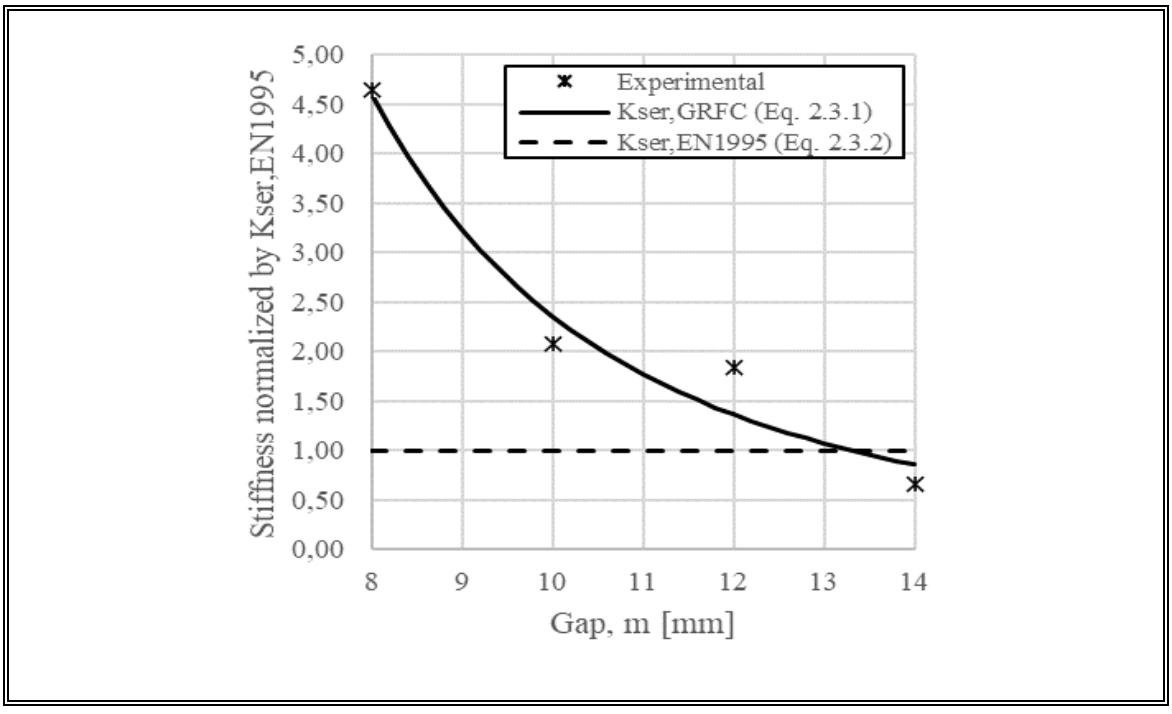

Figure 2-3-4: K_{ser} comparison for EN1995 and GRFC according to gap thickness

All ductility values obtained for all different gap sizes tested in nailed connections were greater than 6.0, allowing the HDG to be classified with a highly ductile behavior

according to Eurocode 8 (European Committee for Standardization, 2004) and the ductility scale proposed by Smith et al. (2006) for timber joints. According to the aforementioned scale, the bolted specimen was however classified with a low ductile behavior because the bolts failed prematurely by shear-off. The increase of ductility in HDG of m = 8 mm, 10 mm, 12 mm and 14 mm, increased by 2.22; 4.71; 2.42 and 1.09 times, respectively, the values recorded for conventional HTT5 hold-down without GRFC, where ductility value reaches 5.90 (Liu & Lam, 2019), while the bolted specimen reached a ductility of just 0.59 times.

2.3.3 Cyclic performance

In this section the experimental results of the cyclic tests of the CN-08-01, CN-08-02, CB-08-01 and CB-08-02 specimens are presented and discussed. Appendix E show the individual results of each test.

2.3.3.1 Influence of the fastener diameter

The HDG cyclic tests (tagged as CN) were calibrated according to a yielding displacement of 0.44 mm, which was obtained from the monotonic results of the MN_08 specimen (m = 8 mm). Figure 2-3-5 shows the load-displacement curves obtained for CN_08_01 (d = 3,76 mm) and CN_08_02 (d = 3,23 mm), which allows for comparing the cyclic performance of different diameters of nails using the same m. The problem of pinching is partially solved. An improvement in dissipative behavior is appreciated for both cases, reflected in wider loops compared to typical loops for timber connections (Quenneville et al., 2018). This improvement is due to the configuration of the GRFC, which simulates the effect of induced plasticization used for moment resistance steel frames through the incorporation of the gap, obtaining hysteresis curves which are closer in shape to those of steel moment frames (Vatansever & Yardimci, 2010).

In Figure 2-3-5, the cumulative energy dissipation at the end of the last cycle for the specimen with fastener diameter of 3.23 mm (CN_08_02) was 22% higher than dissipation obtained for a diameter of 3.76 mm (CN_08_01), showing a better dissipative behavior. In addition, the secant stiffness is on average 20% larger for the first and middle cycles with the use of fasteners of 3.23 mm in diameter, than with the 3.76 mm fasteners, which later converge to the same value r. The increases in energy dissipation capacity and secant stiffness value can be explained due to the number of fasteners used in each specimen. For the CN_08_02 specimen, 40 fasteners were used, while for CN_08_01, only 28 were used. Although both specimens have similar load-carrying capacities, the load distribution along the fasteners was not the same, since in CN_08_02 it was distributed in a total number of fasteners 1.43 times greater than CN_08_01. Also, the tests showed that equivalent viscous damping was higher for CN_08_02, reaching maximum values of 30.8% for the twelfth cycle, with differences from CN_08_01 of 27%.

According to these results, it seems that the use of larger number of thinner fasteners further increases the hysteresis benefits of the GFRC concept, because the thinner fasteners are less prone to embed the reinforcements. Such decrease of embedment in the reinforcement renders less strength and stiffness degradation (less pinching behavior) while keeping higher values of energy dissipation and damping at larger deformations.

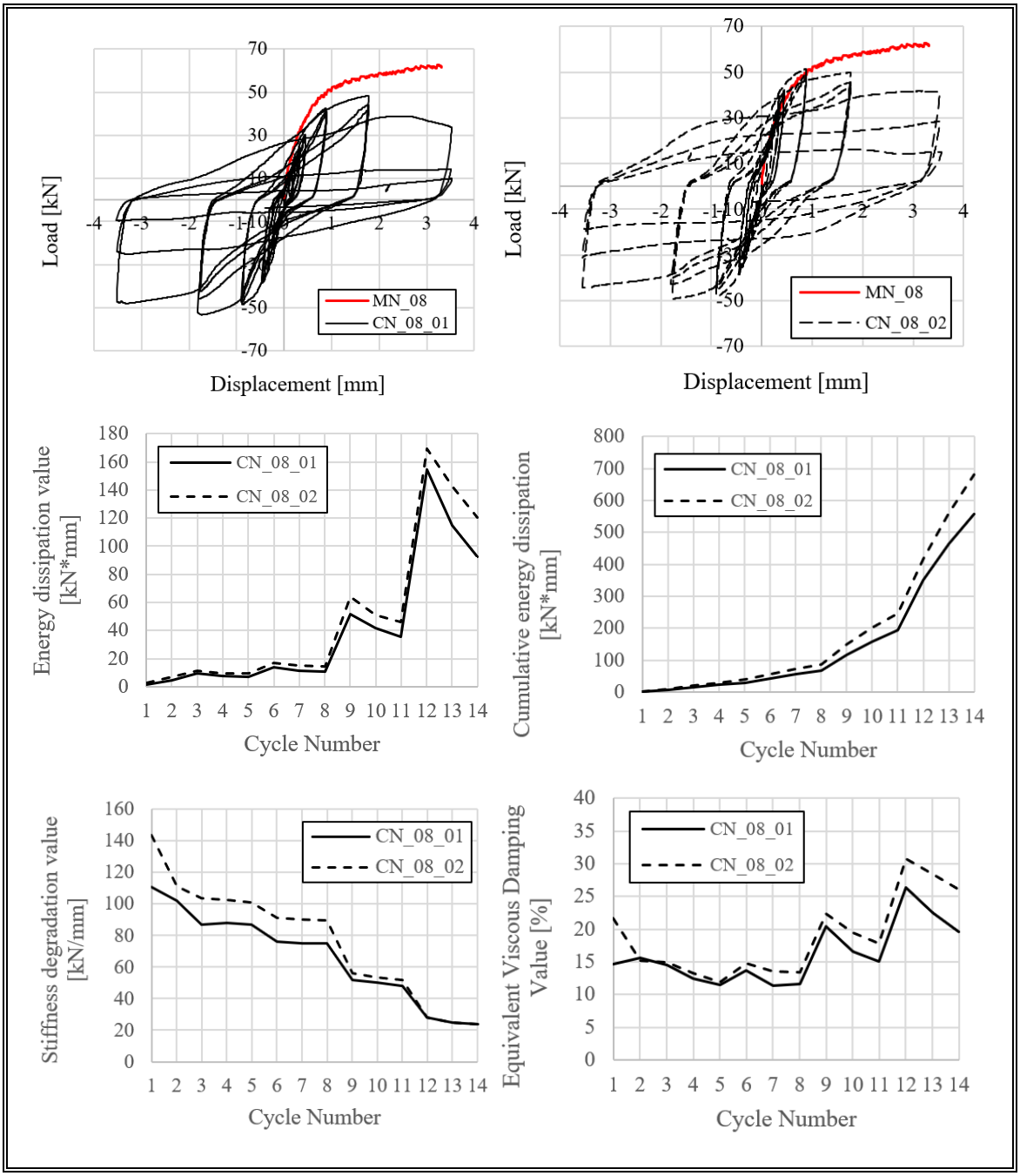

Figure 2-3-5: Nailed cyclic tests results: (From top to bottom, left to right) Load-displacement curves for CN_08_1 (d = 3,76 mm) and CN_08_02 (d = 3,23 mm); Energy dissipation value; Cumulative total energy dissipation; Stiffness degradation; Equivalent viscous damping for each cycle

2.3.3.2 Spacing between fasteners

Bolted GRFC cyclic tests were calibrated for a yielding displacement of 1.68 mm, according to monotonic results for MB_08 specimen. Figure 2-3-6 shows the load-displacement curves obtained for CB_08_01 (longitudinal and edge spacing of 6D) and CB_08_02 (spacing of 4D), which served to assess the cyclic performance of the GRFC concept in terms of potential fastener spacing decrease. In both cases, an improvement was observed with respect to the traditional behavior of timber connections, reflected in less narrowing of the hysteresis loops.

In figure 2-3-6, the cumulative energy dissipation at the end of the last cycle for the specimen with 3D longitudinal spacing (CB_08_02) was 2% higher than dissipation obtained for 6D longitudinal spacing (CB_08_01), showing virtually the same dissipative behavior. On the other hand, secant stiffness increased 11% for the first cycles and on average 22% for middle cycles with the use of 3D spacing. The almost zero variation in energy dissipation can be explained due to the transversal reinforcement provided by the steel plates. In this case, the reinforcing plates, and the timber element to which they were adhered with epoxy, worked as a full composite element. Thus, using the thick plate assumption as well, this allowed the fasteners to exclusively interact with the outer layer of the composite element (i.e., reinforcing steel plates) which in turn allowed for reducing the fastener spacing from the typically large values required in timber structures to those smaller spacings required in steel structures. In fact, for the designed HDG, this interaction took place exclusively between metallic elements (fasteners-plate) and stresses where transferred into the timber tangent stress at epoxied surfaces, thus reducing the spacing requirements between fasteners, which now is being governed by a steel-to-steel interaction according to the design codes for steel elements (American Institute of Steel Construction, 2010). Also, tests showed that equivalent viscous damping is higher for CB_08_02, reaching an average value of 17.5%, with differences from CB_08_01 of 18%.

These results does not only seem promising in reducing the spacing of timber fasteners – which often results in the critical design parameter, for instance in moment resisting connections -, but also may have an unprecedented potential to reduce brittle failure modes at timber members. More specifically, brittle failure risks derived from grouping effects at longitudinal-to-the-grain aligned fasteners as well as perpendicular-to-the-grain concentrated forces cause important drawbacks in timber design. However, with the GRFC concept those brittle risks may be largely avoided because forces can be widely distributed as tangential stresses at the reinforcing plates. Thus, not only the stiffness-ductility behavior can be improved with the GRFC, but also pinching, spacing and brittle failure modes may be considerably enhanced.

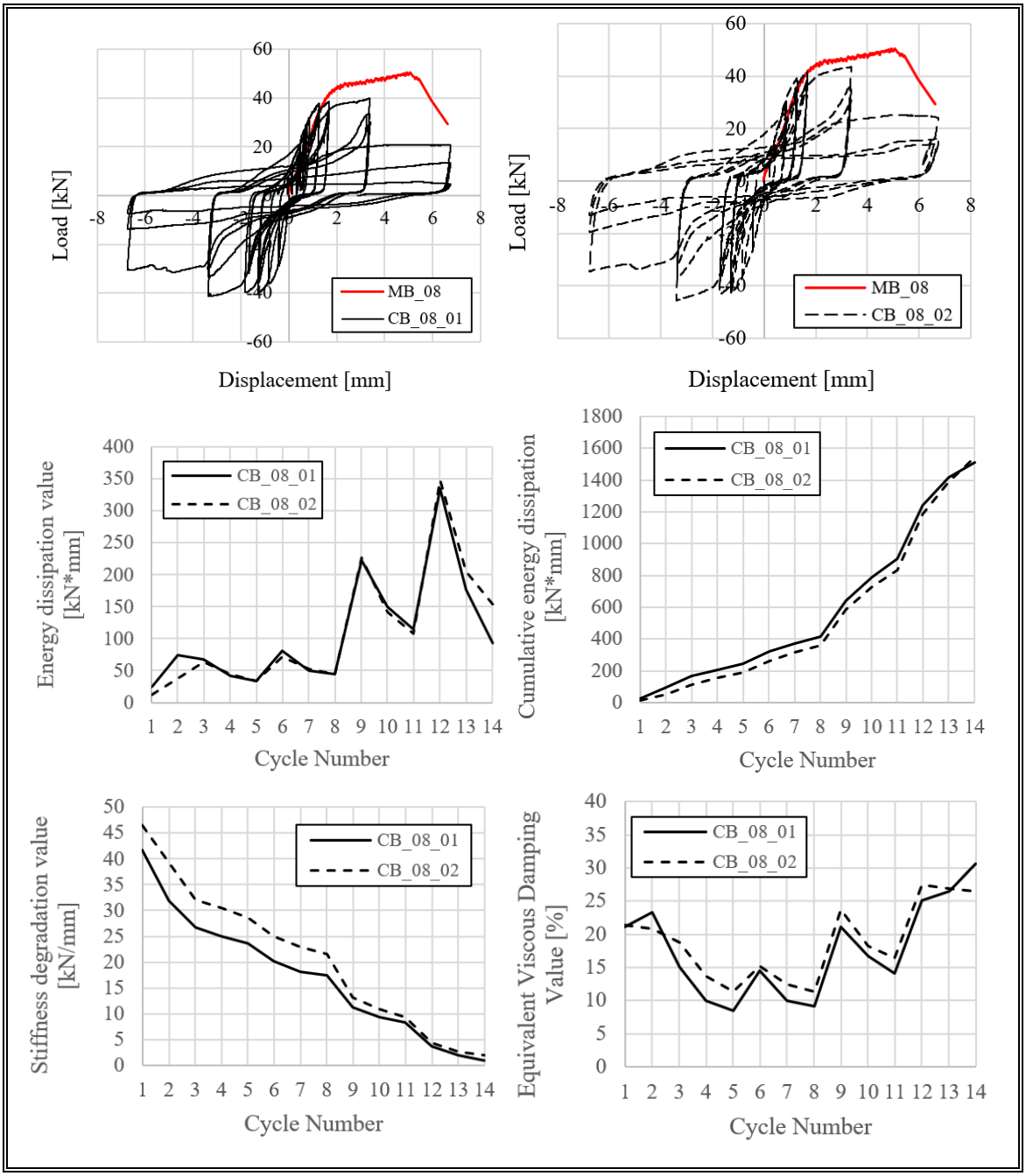

Figure 2-3-6: Bolted cyclic tests results: (From top to bottom, left to right) Load-displacement curves for CB_08_01 (6D spacing, typical from timber structures) and CB_08_02 (3D spacing, typical from steel structure); Energy dissipation value; Cumulative total energy dissipation; Stiffness degradation; Equivalent viscous damping for each cycle

2.3.3.3 Ultimate failure mechanism

Figure 2-3-7 shows the different failure modes registered in the tests. Figure 2-3-7a and Figure 2-3-7b show the yielding of the nails inside the gap area. The development of plastic hinges was more evident for gap sizes of 10 mm, 12 mm and 14 mm, where once the tests were completed the nails remained with their heads intact. However, for a gap size of 8 mm the plasticization of the nails was accompanied by cutting of some of them before the test was finished. For the bolted specimens (Figure 2-3-7c and Figure 2-3-7d), the plasticization of the fasteners was accompanied by shearing of them.

Figure 2-3-8 shows the effects of cyclic loads on CLT and steel plate elements. As can be seen in Figure 2-3-8a and Figure 2-3-8b, drill holes in the wood element remained intact due to the bonded steel reinforcing plate, for both nailed and bolted specimens. Bearing damage was located on the reinforcing steel plates (Figure 2-3-8c and Figure 2-3-8d), due to the development of plastic hinges inside them.

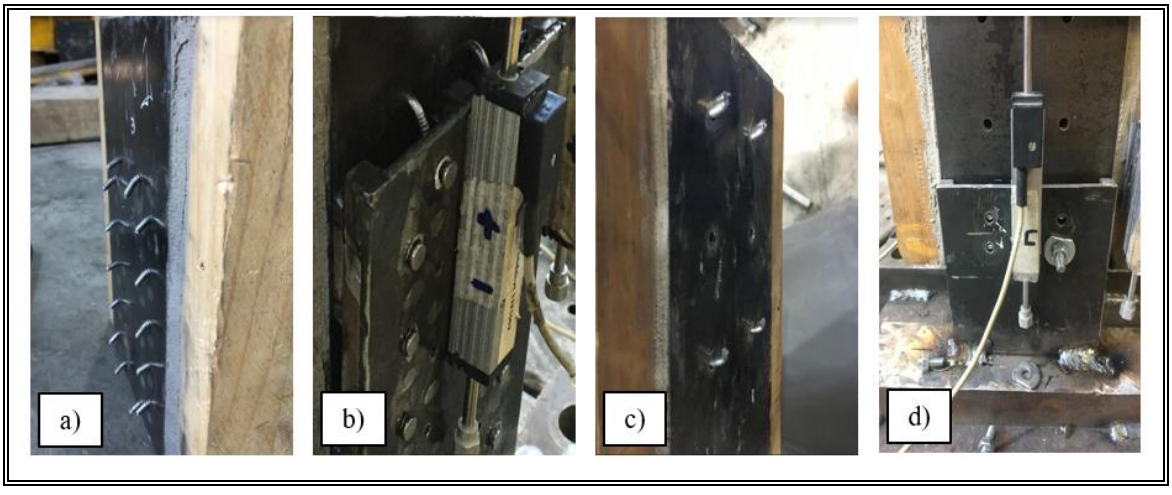

Figure 2-3-7: Failure modes for tested connections: a) MN_08; b) MN_12 (similar for 10 mm and 14 mm gap size); c) MB_08; d) CB_08_02

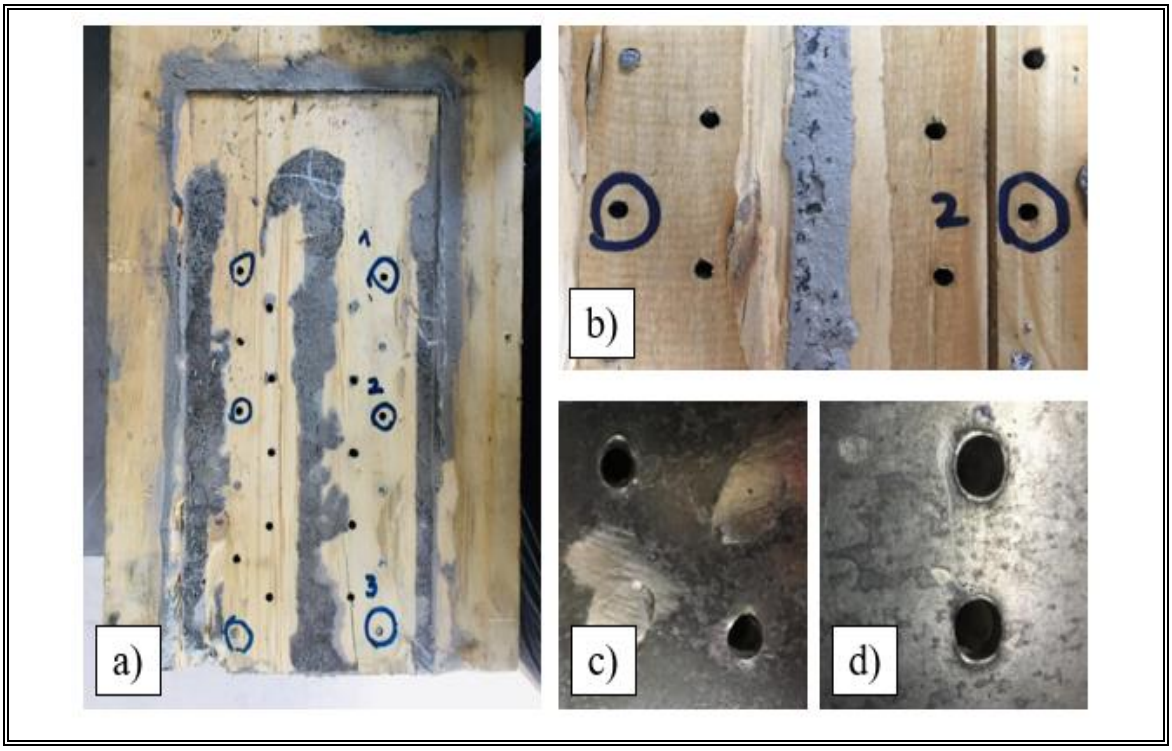

Figure 2-3-8: Crushing on HDG components: a) Perforations in the wood behind the epoxy bonded plate; b) Drill hole zoom on timber element; c) Crushing of steel plate for nailed specimens; d) Crushing of steel plate for bolted specimens

2.3.4 Applications of the GRFC concept

GRFC concept is not only limited to its application in hold-down connections. Additional applications may include connections with high risk of brittle failure modes such as perpendicular-to-grain loaded connections at truss nodes and moment resisting connections where fasteners' spacing is largely restricted. Figure 2-3-9 shows the concept applied to a beam-diagonal connection for diagonally braced lateral systems, where stiffness and ductility are essential for seismic performance.

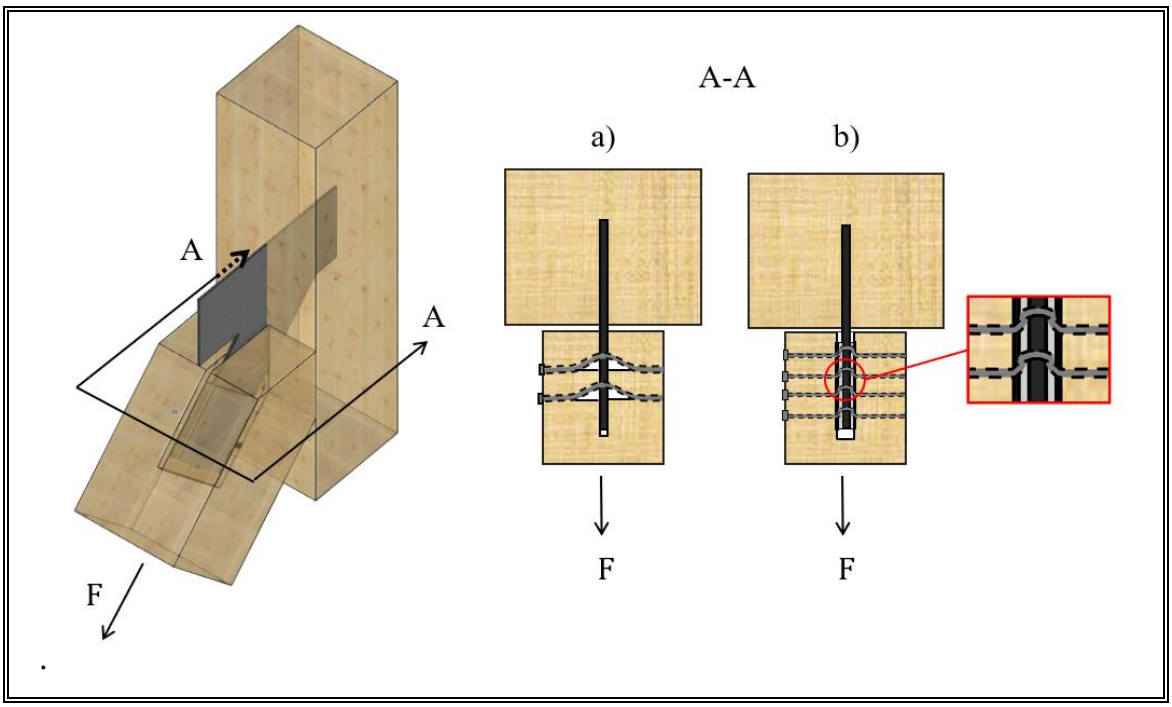

Figure 2-3-9: GRFC concept applied to timber connections for diagonally braced lateral systems (diagonal beam-to-column). a) Crushing of the wood on the diagonal member without GRFC, b) Crushing of reinforcement plate incorporating GRFC concept

3. CONCLUSIONS

In this research, the results of a new reinforced connection concept (GRFC) were presented. Its design allows to obtain a series of improvements in the mechanical behavior compared to traditional connections with mechanical fasteners. Through monotonic tests, it was shown that by incorporating the gap interface, it is possible to obtain the theoretical improvement of the stiffness-ductility ratio of the connection, proposed by the GRFC concept. On the other hand, the cyclic tests show a partial reduction of the pinching effect. Furthermore, these results indicate that the proposed reduction in spacing between the fasteners is possible.

The main conclusions of this research are as follows:

- An improvement in the stiffness-ductility ratio is obtained by modifying the failure mechanism of the connection using GRFC configuration, avoiding the development of plastic hinges of the fasteners inside the wood.

- Using GRFC, a highly ductile and stiff nailed connection is obtained, reaching ductility values up to 4.71 times that of a conventional nailed hold-down connection, while elastic stiffness values reaches up to 3.96 times that of a conventional nailed hold-down connection.

- Using GRFC, a low ductility and stiffness bolted connection is obtained, reaching a ductility value of 0.59 times that of a conventional nailed hold-down connection, while elastic stiffness reaches a value of 0.88 times that of a conventional nailed hold-down connection.

- The stiffness degradation from pinching effect is reduced according to load-displacement curves for the same level of deformation and fastener diameter,

obtaining a load-displacement response similar to a moment resistance steel frame. Energy dissipation is most effective when multiple small diameter connectors are used.

- The elastic stiffness obtained experimentally represents only 10% of the stiffness calculated by the double embedment of the fastener assumption. To predict the stiffness, it is necessary to use a flexibilization factor of 0.1 due to a loss of the fixed end condition between fastener and reinforcing plate.

- The rigid interface provided by the epoxy modifies the spacing requirements, being controlled the failure mode according to the materiality of the external layer of the timber-epoxy-steel composite. It is possible to reduce typical timber connection spacing to those values used in steel connections.

- Spacing reduction and improvement in the ductility-stiffness ratio would allow to redefine the traditional timber connection design used in hold-down type connections, truss nodes, beam-column or moment frame connections, among others.

ACKNOWLEDGEMENTS

The author acknowledges the funding provided by the Fondecyt Project 11170863: “Development of innovative earthquake-resilient shear walls for mid-rise timber construction in Chile” (ANID) and supported by the UC Timber Innovation Center (CIM UC). The specimens were tested in the Laboratory of Structural Engineering laboratory of Pontificia Universidad Católica de Chile.

BIBLIOGRAPHY

American Institute of Steel Construction [AISC]. ANSI/AISC 360-10: Specification for Structural Steel Buildings. English version (2010).

American Society of Civil Engineers [ASCE]. ASTM E2126-11 Standard Test Methods for Cyclic (Reversed) Load Test for Shear Resistance of Vertical Elements of the Lateral Force Resisting Systems for Buildings (2012).

Bejtka, I. (2005). *Verst arkung von Bauteilen aus Holz mit Vollgewindeschrauben* [Reinforcement of timber components with fully threaded screws] (Doctoral thesis). University of Karlsruhe, Germany.

Blaβ, H., Schmid, M., Litze, H. & Wagner, B. (2000). Nail plate reinforced joints with dowel-type fasteners. *World Conference on Timber Engineering 2000*, Whistler, Canada.

Blaβ, H. & Schmid, M. (2001). Self-tapping screws as reinforcement perpendicular to the grain in timber connections. *Joints in timber structures. RILEM Symposium*, Stuttgart, Germany.

Blaβ, H. & Sandhaas, C. (2017). Timber Engineering: Principles for Design. Germany: KIT Scientific Publishing.

Blaβ, H. & Schmidt, T. (2018). Recent development in CLT connections part II: In-plane shear connection for CLT bracing elements under statics loads. *Journal of Wood and Fiber Science, 50*, 58-67.

European Committee for Standardization [CEN]. EN 1998-1: Eurocode 8: Design of structures for earthquake resistance-Part 1: General rules, seismic actions and rules for buildings. English version: EN 1998-1:2004 (2004).

European Committee for Standardization [CEN]. EN 12512: Timber structures-test methods-cyclic testing of joints made with mechanical fasteners. German version: EN 12512:2001+A1:2005 (2005).

European Committee for Standardization [CEN]. EN 1995-1-1: Eurocode 5: Design of timber structures-Part 1-1: General – Common rules and rules for buildings. German version: EN 1995-1-1:2004+AC:2006+A1:2008 (2010).

Izzi, M. & Polastri, A. (2019). Low cycle ductile performance of screws used in timber structures. *Journal of Construction and Building Materials*, *217*, 416-426.

Johansen, K. (1949). Theory of timber connections. *International Association for Bridge and Structural Engineering, 9,* 249-262.

Kelly, J., Skinner, R. & Heine, A. (1972). Mechanisms of energy absorption in special devices for use in earthquake-resistant structures. Society for Earthquake Engineering, *5*(3), 63-88.

Larson, G. (2019). *The shear plate dowel joint: Research on a novel connection for heavy timber structures* (Doctoral thesis). Department of Construction Sciences, Lund University, Sweden.

Liu, J. & Lam, F. (2019). Experimental test of coupling effect on CLT hold-down connections. *Journal of Engineering Structures*, 178, 586-602.

Popov, E., Tzong, Y. & Shih, C. (1998). Design of steel MRF connections before and after 1994 Northridge earthquake. *Journal of Engineering Structures*, *20*(12), 1030-1038.

Quenneville, P., Chan, N. & Zarnani, P. (2018). Pinching-free timber connections-opening up new possibilities for timber structures resisting earthquakes. *World Conference on Timber Engineering 2018*, Seoul, Republic of Korea.

Schädle, P., Blaβ, H. (2011). Ductility aspects of reinforced and non-reinforced timber joints. *Journal of Engineering Structures, 33,* 3018-3026.

Scotta, R., Marchi, L., Trutalli, D. & Pozza, L. (2016). A Dissipative Connector for CLT Buildings: Concept, Design and Testing. *Materials, 9*(3), 139.

Simpson Strong-Tie (2019). Wood Construction Connectors C-C-2019. 54-55.

Smith, I., Asiz, A., Snow, M. & Chui, I. (2006). Possible Canadian/ISO approach to deriving design values from test data. *39th CIB Working Commission W18-Timber Structures*, University of Karlsruhe, Germany.

Tomasi, R., Crosatti, A. & Piazza, M. (2010). Theoretical and experimental analysis of timber-to-timber joints connected with inclined screws. *Journal of Construction and Building Materials*, *24*, 1560-1571.

Vatansever, C. & Yardimci, N. (2010). Cyclic behavior and numerical modelling of a semi-rigid frame. *Journal of Steel Construction, 3*(3), 128-133.

APPENDICES

APPENDIX A: DENSITY VALUES FOR THE TEST SPECIMENS

Density values for tests in Table 2-2-1. For the calculation of the density, only the mass and volume values associated with the wood are considered, the steel elements (reinforcement plates) are excluded.

Table A.1: Wood density for the test specimens

Test	**Density [kg/m^3]**
MN-08	474,7
MN-10	479,5
MN-12	466,2
MN-14	434,2
MB-08	509,1
CN-08-01	473,5
CN-08-02	469,1
CB-08-01	452,2
CB-08-02	442,4

Average:	**466,78**
Standard dev.:	22,18
C.V.:	0,05

APPENDIX B: INSTRUMENTATION OF CONNECTION TESTS

Detailed instrumentation for connection tests.

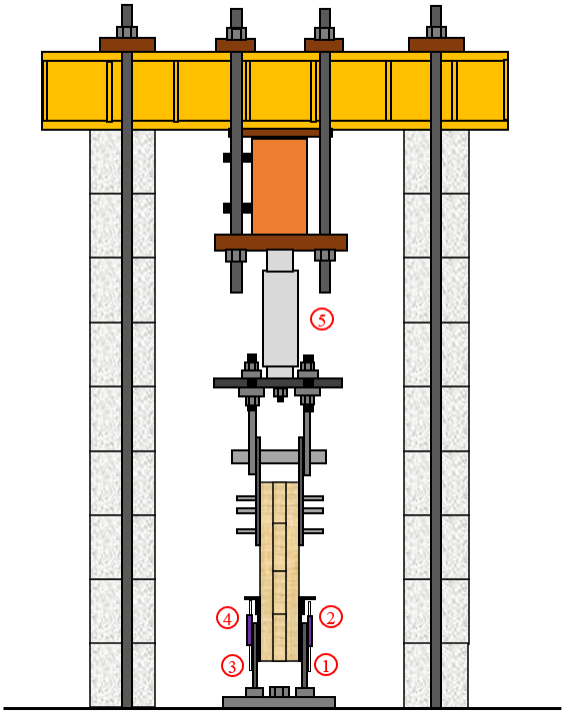

1. Relative displacement between left epoxied steel plate reinforcement and external steel plate, measured with a linear variable displacement transformer (LVDT).
2. Zero control between left epoxied steel plate reinforcement and CLT, measured with a linear variable displacement transformer (LVDT).
3. Relative displacement between right epoxied steel plate reinforcement and external steel plate, measured with a linear variable displacement transformer (LVDT).
4. Zero control between right epoxied steel plate reinforcement and CLT, measured with a linear variable displacement transformer (LVDT).
5. Monotonic/cyclical load application, measured with a load cell.

Figure B.1: Test setup for the connections tests

APPENDIX C: LOAD-DISPLACEMENT CURVES FOR MONOTONIC TESTS

Load-displacement curve obtained according to EN 12512 monotonic procedure. The stopping criterion for each test is shown in Table C.1.

Table C.1: Stopping criterion for the test specimens.

Test	Stopping criterion
MN-08	80% of the maximum load
MN-10	80% of the maximum load
MN-12	80% of the maximum load
MN-14	80% of the maximum load
MB-08	Failure of fasteners

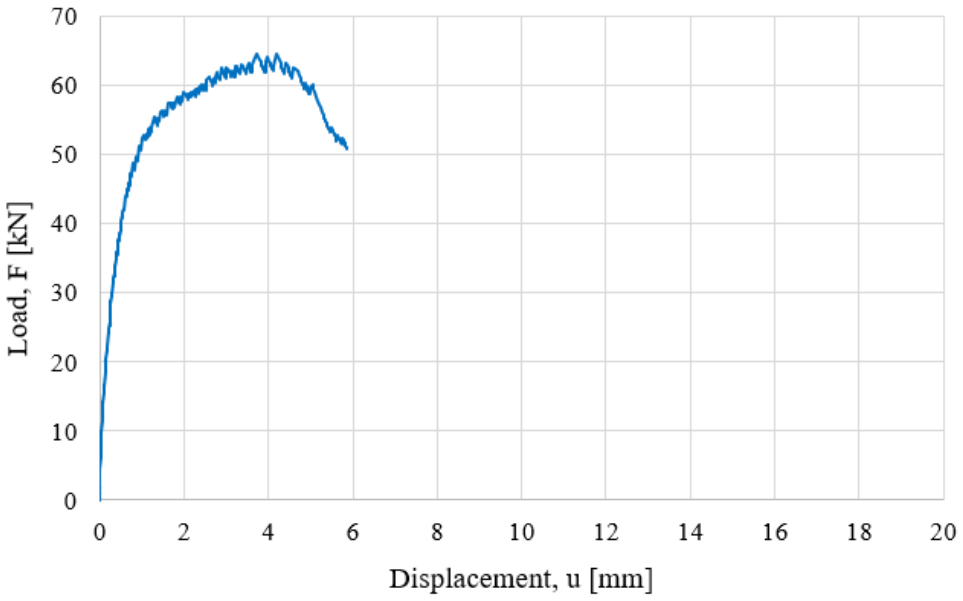

Figure C.1: Load displacement curve for MN-08.

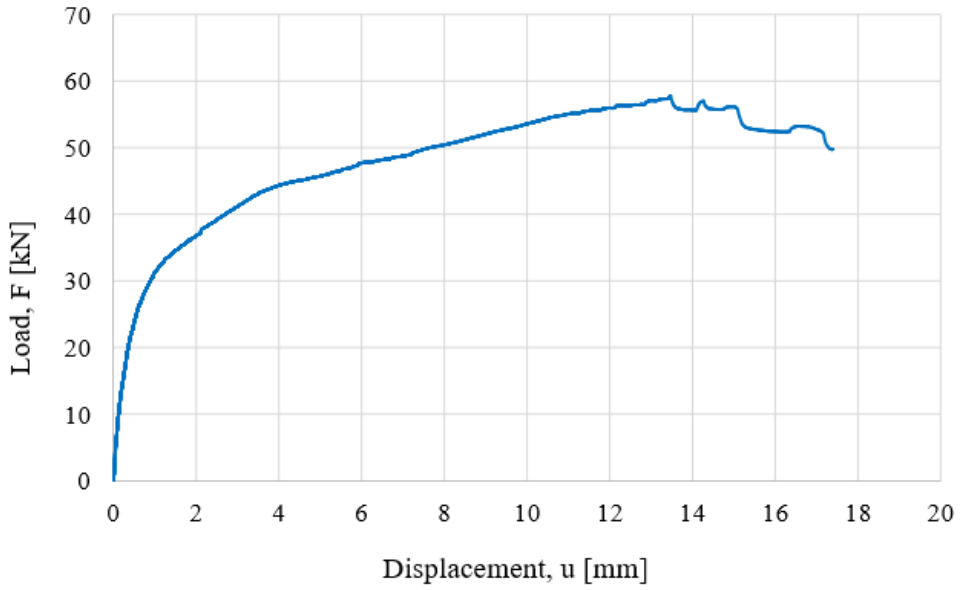

Figure C.2: Load displacement curve for MN-10.

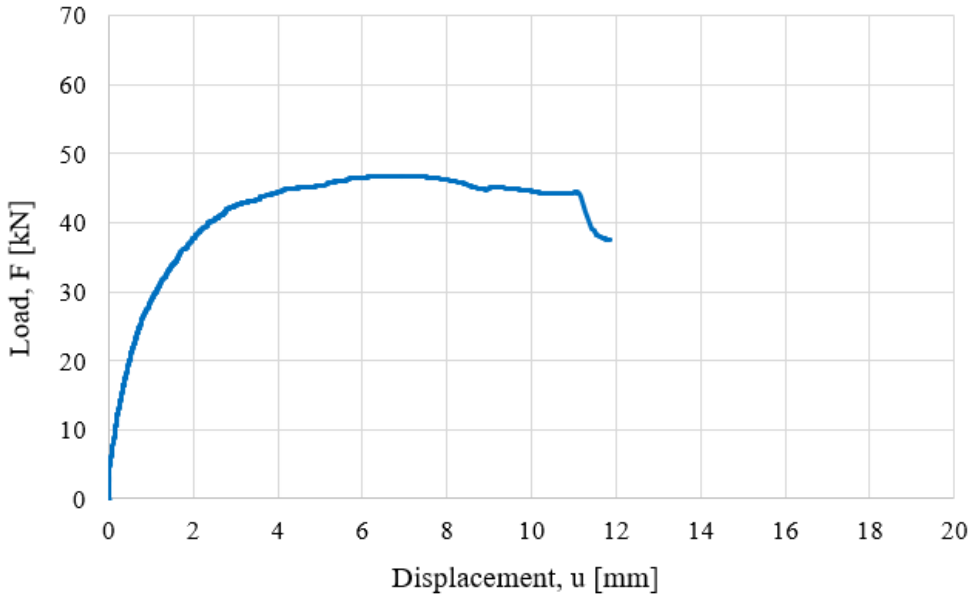

Figure C.3: Load displacement curve for MN-12.

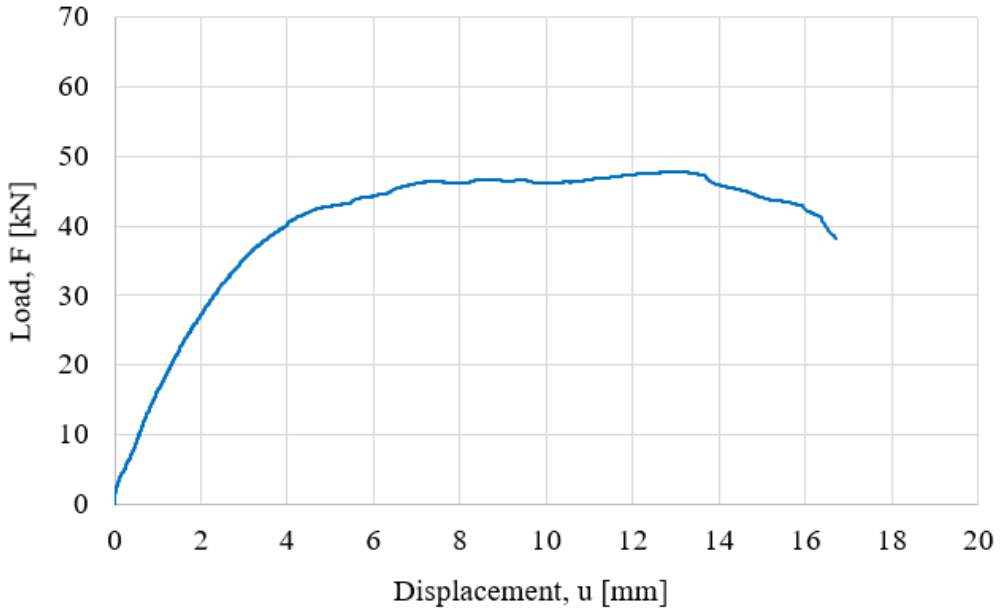

Figure C.4: Load displacement curve for MN-14.

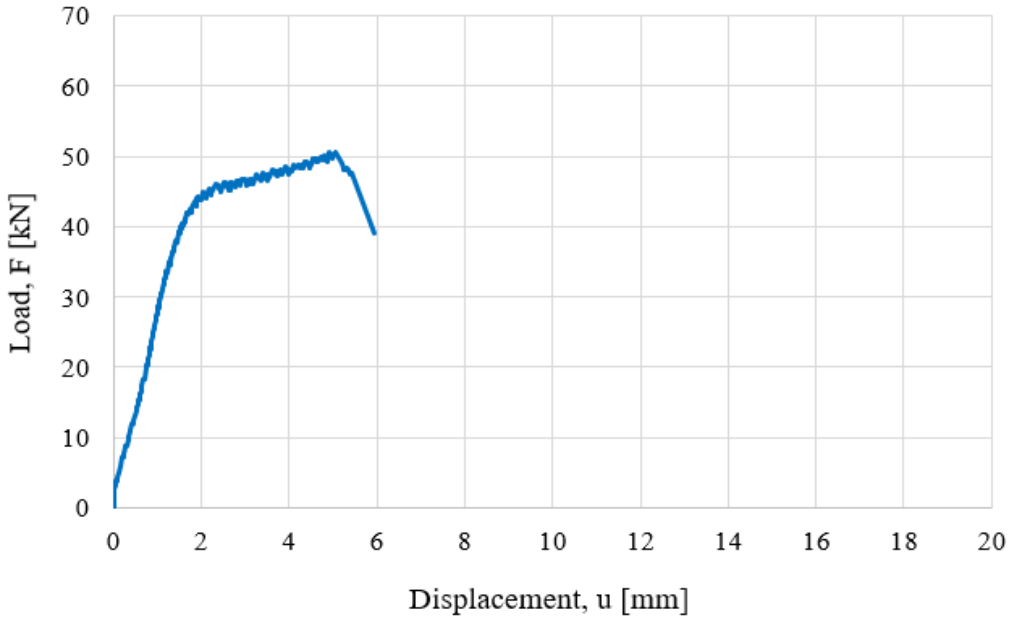

Figure C.5: Load displacement curve for MB-08.

APPENDIX D: CALCULATION OF YIELDING PARAMETERS

Yielding displacement and load according ASTM E2126-11 and EN 12512.

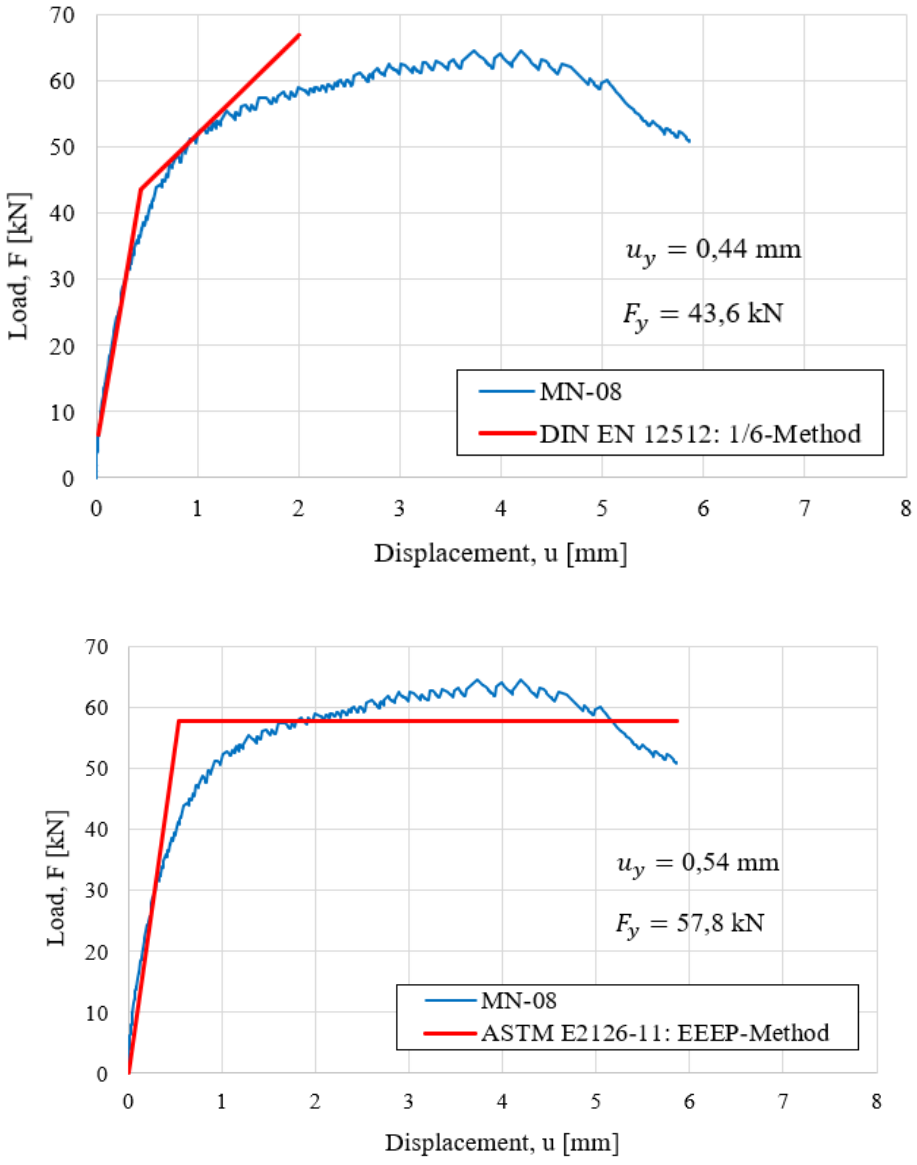

Figure D.1: Yielding parameters estimation for MN-08. DIN EN 12512: 1/6-Method (top), ASTM E2126-11: EEEP-Method (bottom).

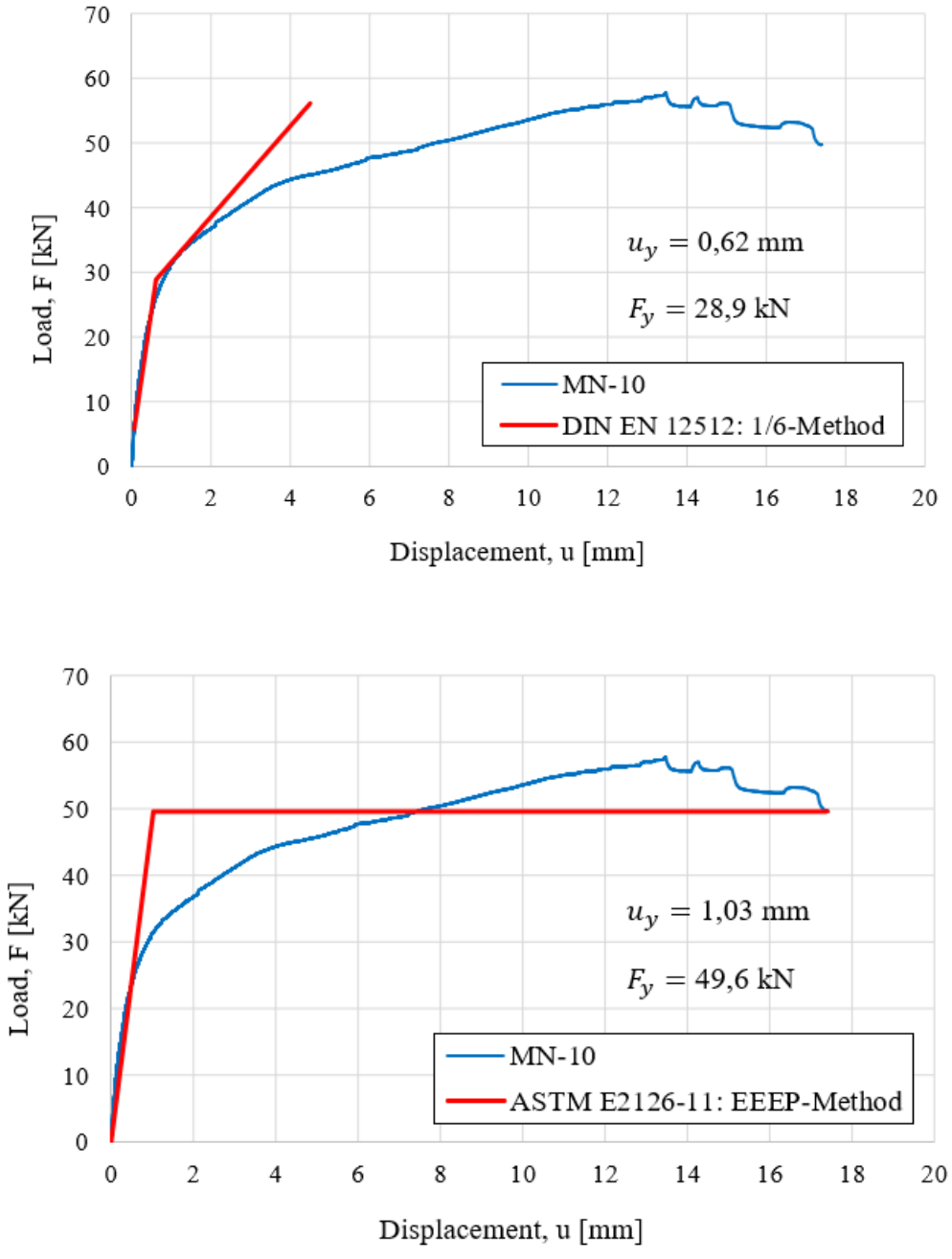

Figure D.2: Yielding parameters estimation for MN-10. DIN EN 12512: 1/6-Method (top), ASTM E2126-11: EEEP-Method (bottom).

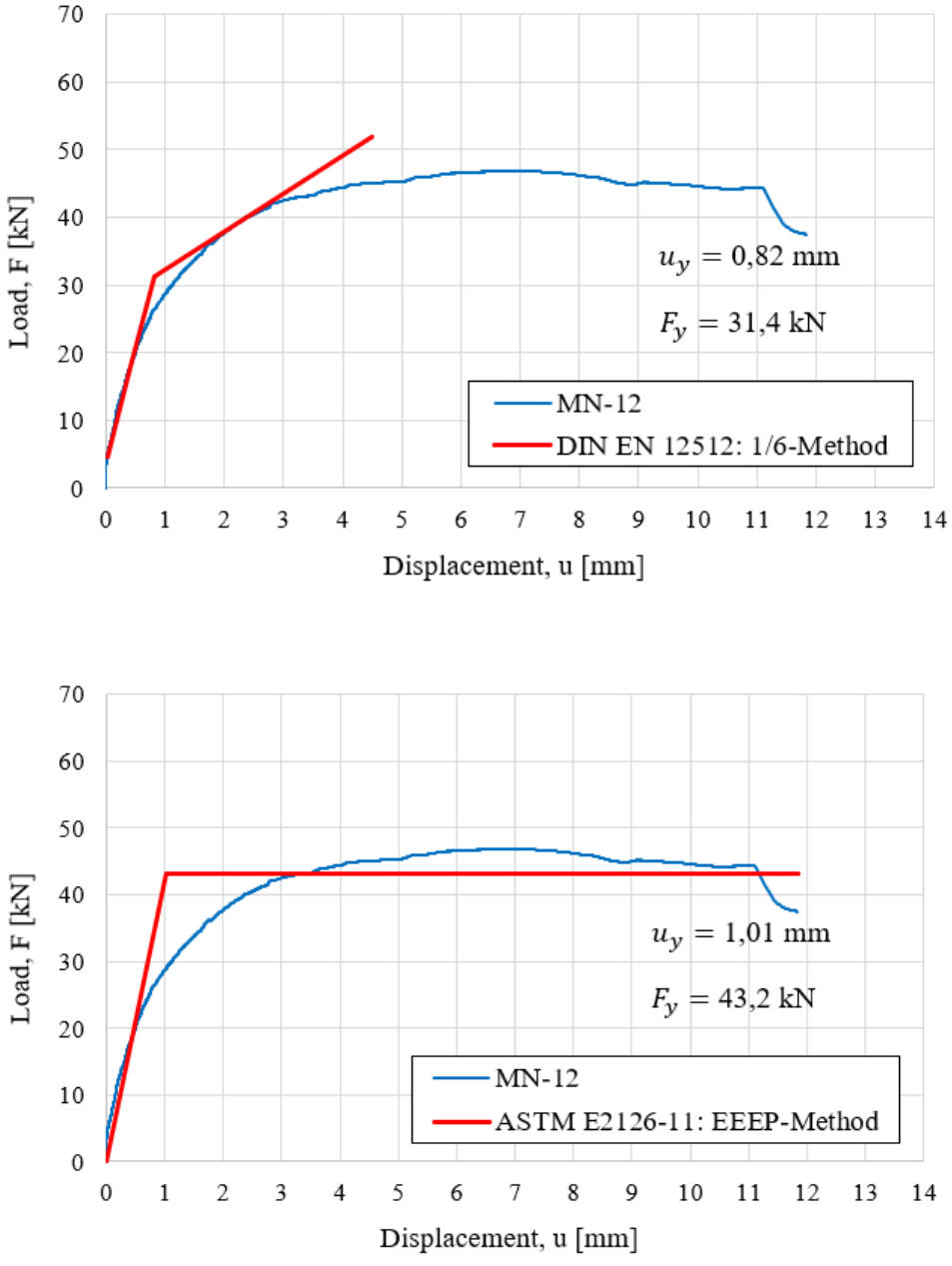

Figure D.3: Yielding parameters estimation for MN-12. DIN EN 12512: 1/6-Method (top), ASTM E2126-11: EEEP-Method (bottom).

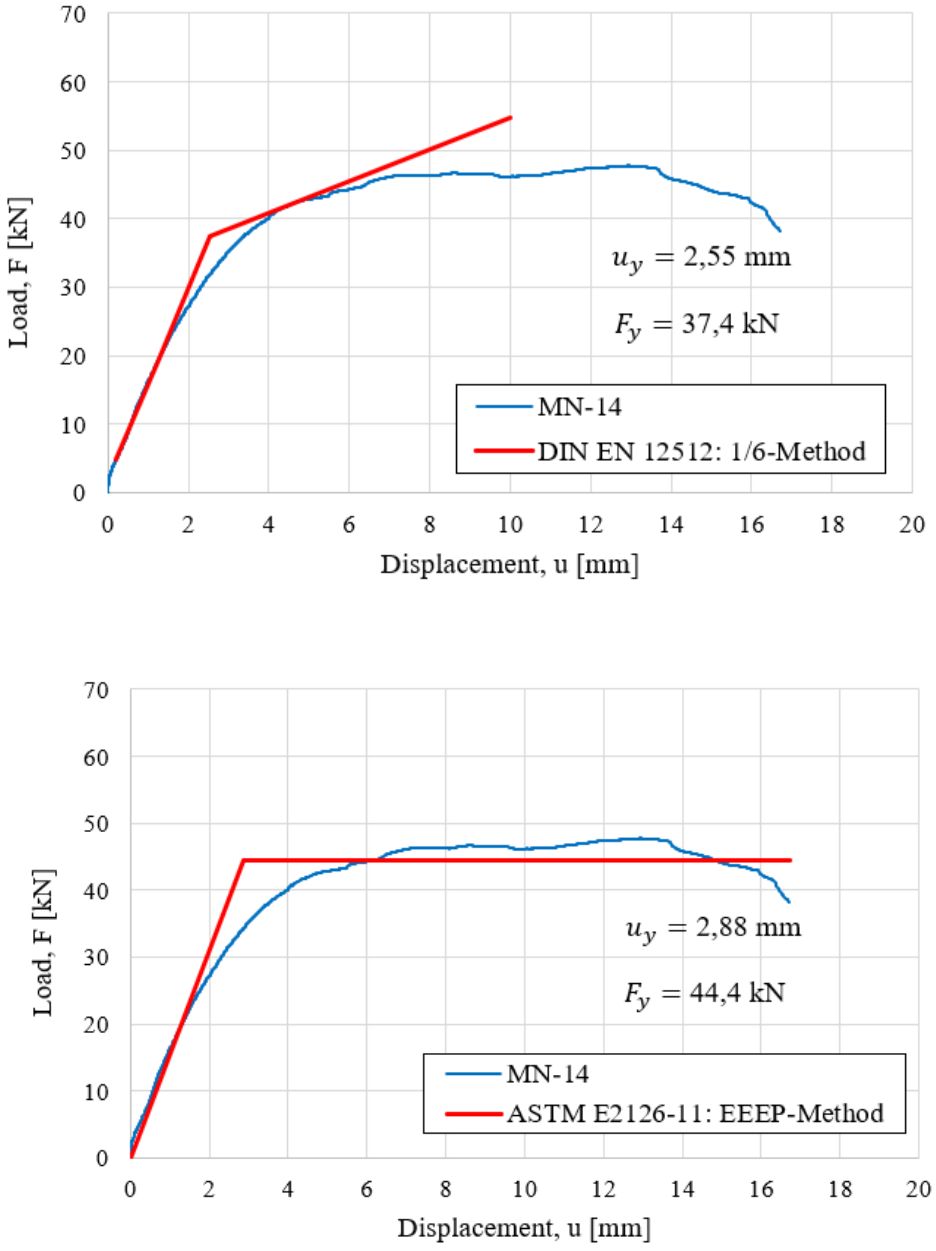

Figure D.4: Yielding parameters estimation for MN-14. DIN EN 12512: 1/6-Method (top), ASTM E2126-11: EEEP-Method (bottom).

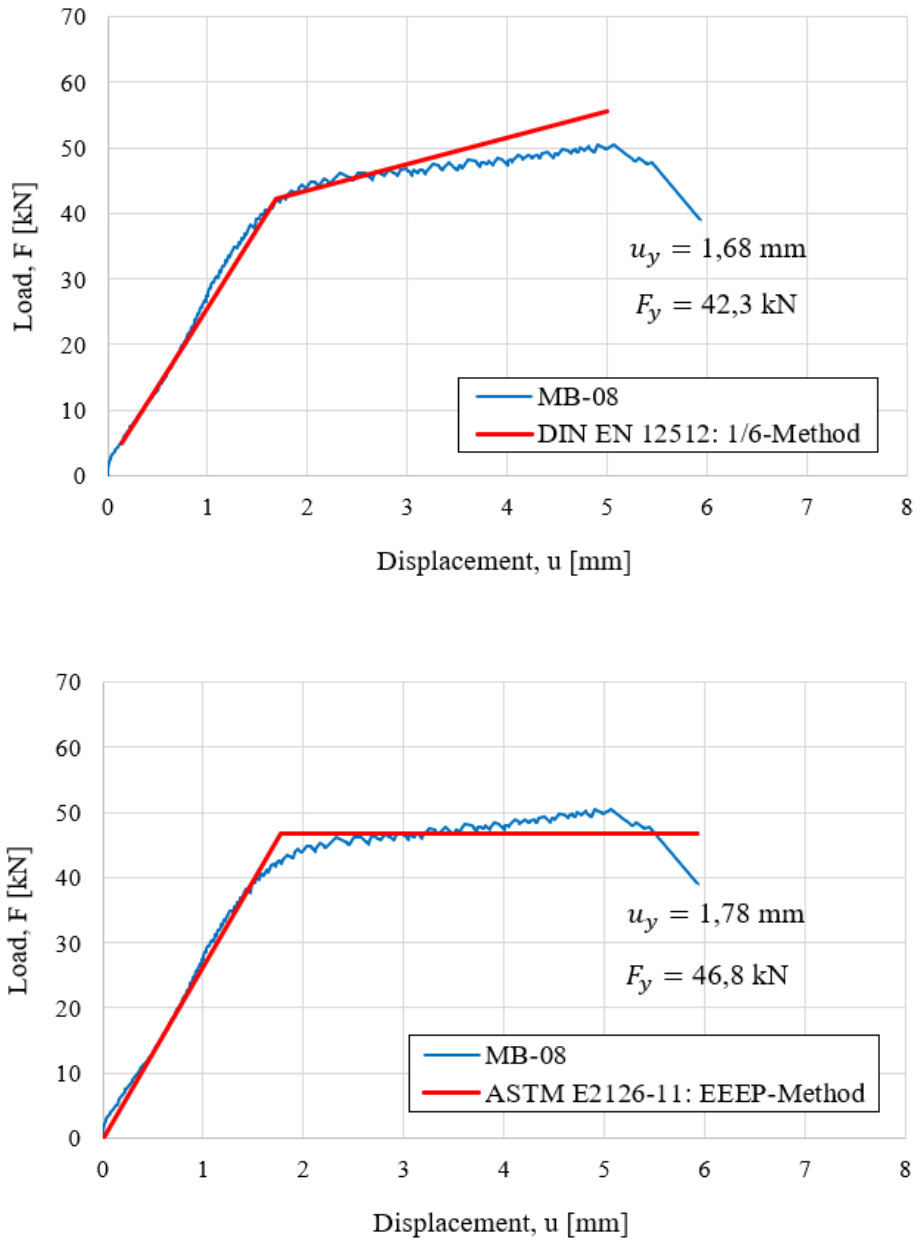

Figure D.5: Yielding parameters estimation for MB-08. DIN EN 12512: 1/6-Method (top), ASTM E2126-11: EEEP-Method (bottom).

APPENDIX E: LOAD-DISPLACEMENT CURVES FOR CYCLIC TESTS

Load-displacement curve obtained according to EN 12512 cyclic procedure.

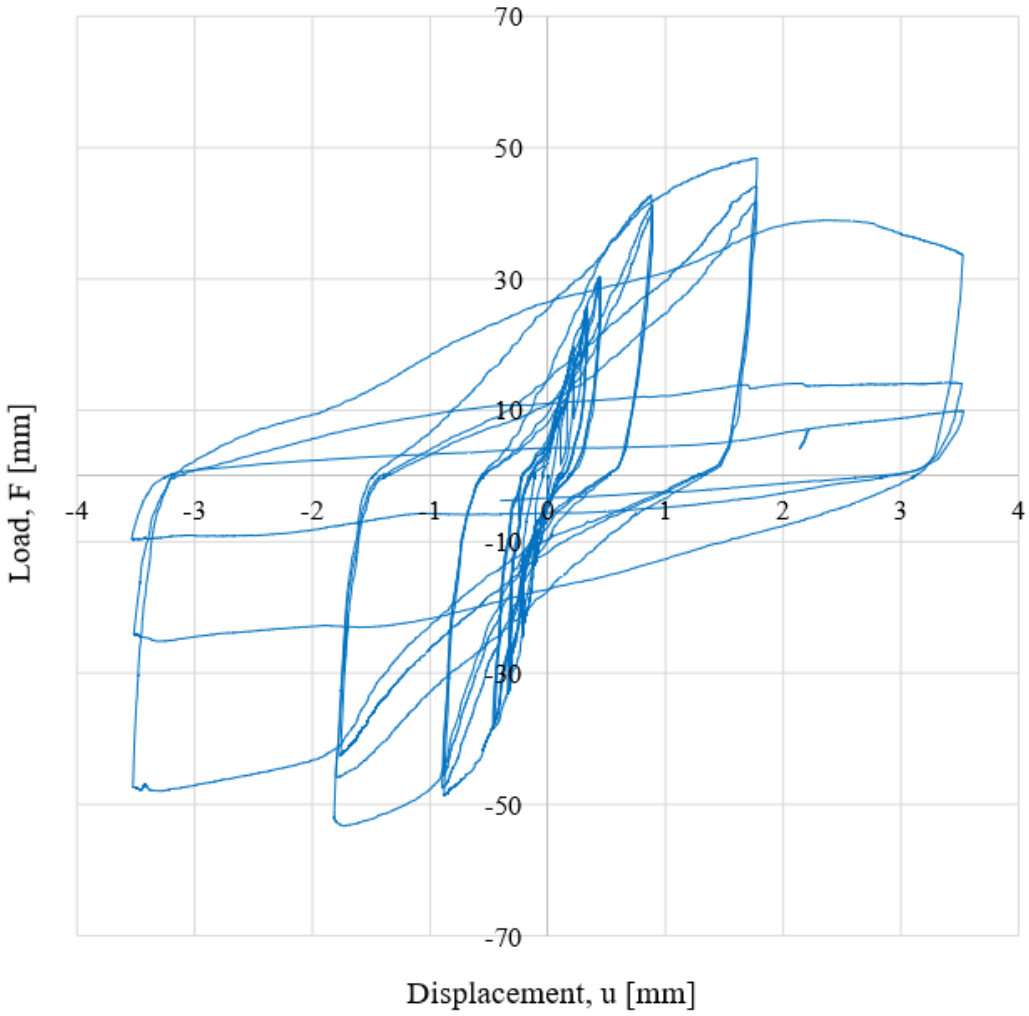

Figure E.1: Load displacement curve for CN-08-01.

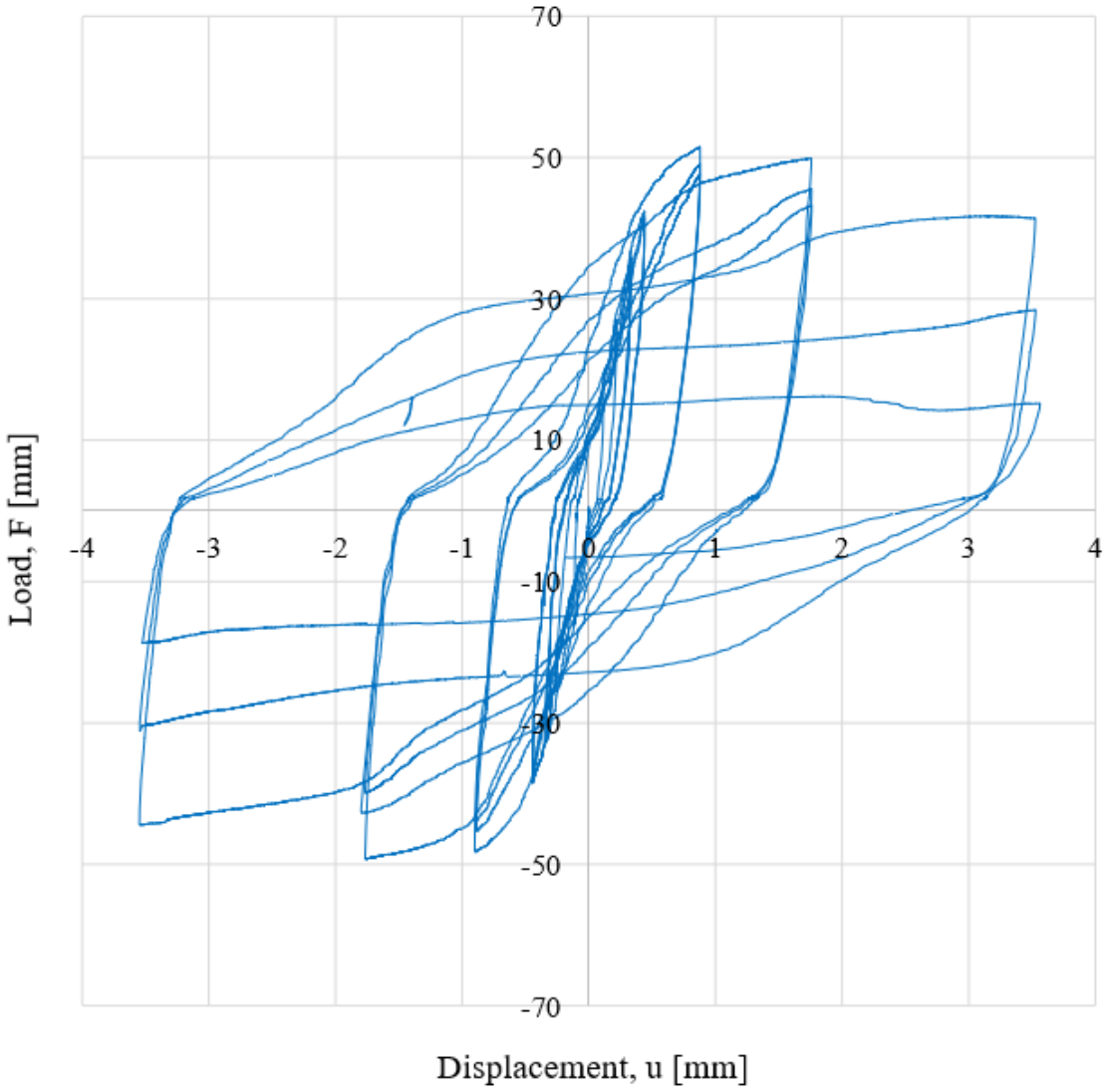

Figure E.2: Load displacement curve for CN-08-02.

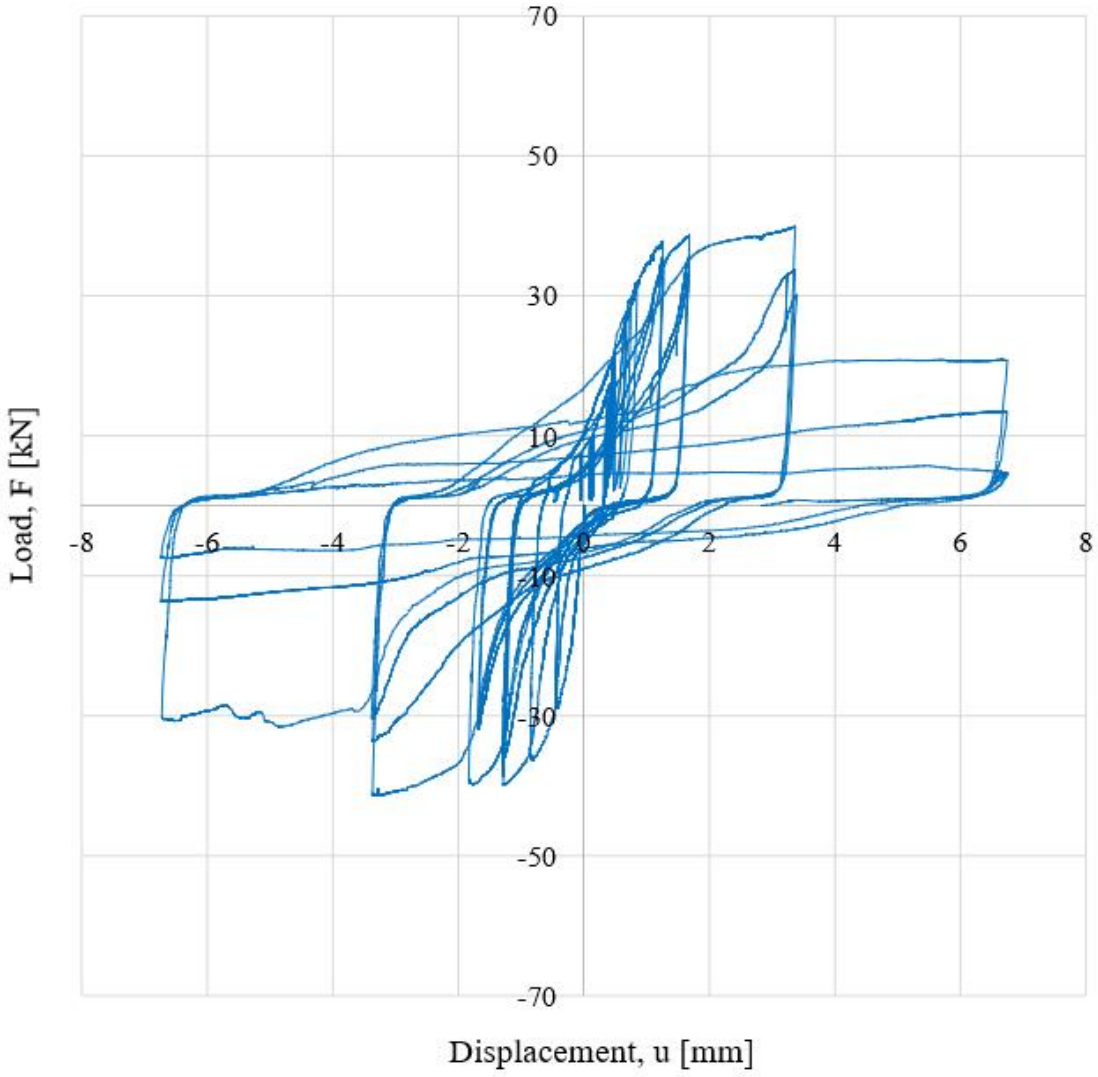

Figure E.3: Load displacement curve for CB-08-01.

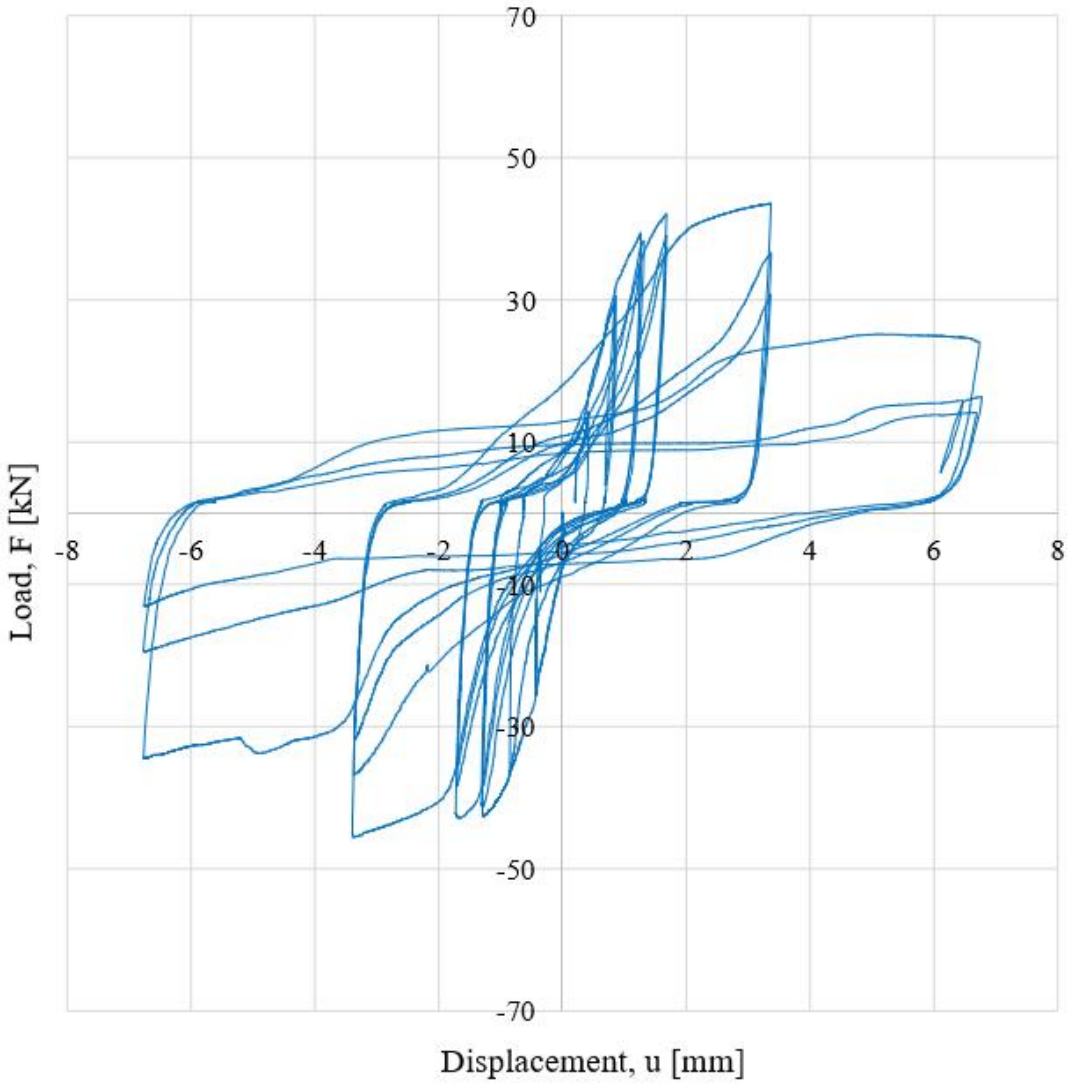

Figure E.4: Load displacement curve for CB-08-02.